How curtailment affects the spatial allocation of variable renewable electricity - What are the drivers and welfare effects?

AUTHOR

Dominic Lencz

EWI Working Paper, No 23/02

Initial publication: March 2023
Revised edition: April 2024

Institute of Energy Economics at the University of Cologne (EWI)
www.ewi.uni-koeln.de

Institute of Energy Economics
at the University of Cologne (EWI)

Alte Wagenfabrik
Vogelsanger Str. 321a
50827 Köln
Germany

Tel.: +49 (0)221 277 29-100
Fax: +49 (0)221 277 29-400
www.ewi.uni-koeln.de

CORRESPONDING AUTHOR

Dominic Lencz

ISSN: 1862-3808

How curtailment affects the spatial allocation of variable renewable electricity - What are the drivers and welfare effects?

Dominic Lencz[a,*]

[a] *Institute of Energy Economics, University of Cologne, Vogelsanger Straße 321a, 50827 Cologne, Germany.*

Abstract

Variable renewable electricity (VRE), generated for instance by wind or solar power plants, is characterised by negligible variable costs and an availability that varies over time and space. Locating VRE capacity at sites with the highest average availability maximises the potential output. However, potential output must be curtailed, if system constraints prevent a local use or export. Such system constraints arise from the features defining the system, which I denote as system topology. Therefore, site choices that are unfavourable from a potential output perspective may still be optimal from a total system cost perspective. Previous research has shown that first-best investments require nodal prices that take account of the system constraints. Market designs that do not reflect nodal prices, such as uniform pricing, typically fail to achieve optimal site choices. However, a profound theoretical understanding of the economic trade-offs involved in the optimal spatial allocation of VRE is lacking. My paper contributes to filling this research gap. To do so, I develop a highly stylised model in which producers, taking into account the system topology, allocate VRE capacity in a one-shot game. Using the model, I analytically show that the optimal spatial allocation can be grouped into three spatial allocation ranges. Which of these ranges applies, I find to be highly dependent on the system topology parameters. In the first range, valid for relatively low VRE penetration levels, it is optimal to allocate all capacity to the node with the higher average availability. In the second and third range, it is optimal to allocate marginal capacity either fully or partially to the node with the lower average availability, i.e., the less favourable site from a potential output perspective. For uniform pricing, I show that producers allocate capacity inefficiently when VRE penetration exceeds a certain threshold. The resulting welfare losses I find to be especially high when transmission capacity is low, the difference in average VRE availability is large, and demand is concentrated at the node with the lower availability.

Keywords: variable renewable electricity, spatial allocation, nodal pricing, uniform pricing, theoretical analysis
JEL classification: Q42, Q48, D47

* *E-mail address*: dominic.lencz@gmx.de

1. Introduction

Variable renewable electricity (VRE), generated for instance by wind or solar power plants, is characterised by negligible variable costs. Another characteristic is that the availability of VRE sources is determined by external factors, such as wind speed or solar radiation, which vary over time and space. The product of the availability and the installed capacity defines the potential supply. If the potential supply can neither be used locally nor exported, it must be curtailed. Such electricity, which could be provided free of charge, cannot be used to generate welfare. In the year 2020, according to Yasuda et al. (2022), less than five percent of the potential supply of VRE was curtailed in most countries. However, curtailment is found to increase as VRE increases in several markets in Europe, America and Asia. In Ireland and Denmark, where VRE from wind already meets 35% and 45% of demand respectively, curtailment reaches 11% and 8% (Yasuda et al., 2022). The increase in curtailment is plausible because, as VRE penetration increases, VRE production more often exceeds demand and must be curtailed when it cannot be exported or stored. Sinn (2017), who extrapolates the German VRE penetration, finds that curtailment increases exponentially if no additional measures are taken. When the VRE share doubles from 30% to 60%, VRE curtailment is found to increase from zero to 16%. For a VRE share of 90%, more than 60% of the total potential VRE supply is curtailed in the analysis of Sinn (2017). In other words, meeting 90% of demand with VRE would require capacity with a potential supply of more than 200% of demand. These figures highlight the increasing importance of curtailment in the context of VRE expansion.

To maximise welfare, curtailment should be reduced to an appropriate level: An appropriate level of curtailment balances the costs of curtailment and the costs of mitigating curtailment. The costs of curtailment arise from actions which compensate for the curtailed electricity, such as investing in additional VRE capacity. The costs of mitigating curtailment occur from actions which mitigate curtailment. Actions to mitigate curtailment are investments in storage and demand flexibility (e.g., Sinn, 2017; Zerrahn et al., 2018; Müller, 2017), network expansion (e.g., Fürsch et al., 2013), or a network-friendly allocation of VRE (e.g., Schmidt and Zinke, 2020). In this paper, I focus on the relationship between curtailment and the spatial allocation of VRE.

The spatial allocation decision when investing in VRE is driven by potential supply. As the weather differs between sites, the potential supply of VRE differs. Placing VRE capacity at sites with the highest availabilities maximises the potential supply. However, it is well known in the literature that system constraints may imply that unfavourable site choices from a potential supply perspective may still be optimal from a total system cost perspective (e.g., Schmidt and Zinke, 2020; Green, 2007; Obermüller, 2017; Pechan, 2017). The

system constraints and their relevance are likely to depend on the features of the system. In the remainder of the text, I denote the features of the system as system topology. For VRE, relevant parameters describing the system topology are the transmission capacity, the spatial distribution of demand, the VRE penetration, the correlation, the average and the variance of VRE availabilities, as well as the capacities of storage and demand flexibility. Similar observations regarding the effect of the spatial allocation on the total system costs apply to any investment in generation, storage, or demand (e.g., Green, 2007; Czock et al., 2022; Müller, 2017). Therefore, it has been shown that first best investments require nodal prices that take into account system constraints arising from the system topology (Schweppe et al., 1988). Vice-versa, it follows, and has been demonstrated in numerous case studies, that market designs which do not reflect nodal prices, such as uniform pricing, typically fail to identify optimal site choices (e.g., Schmidt and Zinke, 2020; Green, 2007; Obermüller, 2017; Pechan, 2017).

Against this backdrop, I shed more light on the impact of various parameters of the system topology on the spatial allocation of VRE in the social optimum and under uniform pricing. The existing literature lacks a comprehensive understanding of these issues. Instead, most papers analyse either the effect of single system topology parameters or the effect of the market design, i.e. nodal versus uniform pricing. In addition, most studies consider a specific real-world setting. For example, Elberg and Hagspiel (2015) analyse the effect of increasing VRE penetration on the market value of VRE for the case of Germany. The authors find that market values decrease most for regions with high availability, suggesting that for high VRE penetration, it may be welfare-enhancing to allocate some capacity to regions with average or low availability. Schmidt and Zinke (2020) analyse the spatial allocation of wind capacity in Germany under nodal and uniform pricing for investments in the years 2020 to 2030. The authors find that 95% of the wind capacity added is allocated inefficiently, resulting in a welfare loss of 1.5% in terms of variable production costs. The most comprehensive analysis is provided by Pechan (2017). She analyses the impact of the correlation, the average and the variance of VRE availability on spatial allocation. She calculates the allocation in the social optimum and under uniform pricing and considers a 6-node network. Pechan (2017) finds that, under nodal pricing, producers increasingly concentrate capacity at high-availability nodes when the correlation increases and when the variance in the high-availability node is low. However, Pechan (2017) only analyses a setting where VRE serve 50% of demand, and she does not vary the transmission capacity or the demand distribution. She also performs a numerical analysis with few scenarios. Therefore, her results cannot be generalised.

To contribute to closing the research gap I analyse the following research questions:

1. From a theoretical perspective, under which states of the system topology is it welfare-enhancing to allocate some VRE capacity to sites with unfavourable potential supply?
2. How does the spatial allocation differ between a uniform pricing regime and a first-best nodal pricing regime, and what are the resulting welfare effects?

To analyse these research questions, I develop a stylised theoretical model. The model depicts the spatial allocation of VRE sources in a two-node network with limited transmission capacity. At the two nodes, consumers have a constant demand that must be satisfied by producers who can use a conventional and a VRE technology. The central element of the model is that producers decide how to spatially allocate VRE capacity. I model the spatial allocation of all VRE capacity as a one-shot game where producers consider a specific system topology, i.e. one specific configuration of transmission capacity, spatial distribution of demand, VRE penetration and VRE availability. This differs from reality, where VRE penetration and other system topology parameters dynamically evolve over time. The implications of assuming a one-shot game I discuss in Chapter 5. The model considers availabilities which vary over time and between the nodes. The temporal sequence of availabilities I refer to as availability profile. The average availability I assume to be higher in one node (i.e. high-availability node) compared to the other node (i.e. low-availability node). The effect of storage and demand flexibility I do not analyse in the model itself to ensure an analytical solution. The analytical solution is crucial to gain a profound theoretical understanding. To still shed light on the effect of storage and demand flexibility, I discuss the effects qualitatively based on the model results and findings from other papers in Chapter 5. To analyse the relationship between spatial allocation under a first-best nodal pricing regime and a uniform pricing regime, I solve the model for both market designs.

The main findings of the analysis regarding the first research question are as follows: The optimal spatial allocation can be grouped into three spatial allocation ranges that are valid for different levels of VRE penetration. For low levels of VRE penetration, all VRE capacity should be allocated to the high-availability node (i.e. *high-availability deployment range*). For such levels of VRE penetration, it is not welfare-enhancing to allocate some VRE capacity to sites with unfavourable potential supply. For higher levels of VRE penetration, resulting in curtailment that eliminates the advantage arising from higher average availability, it is optimal to allocate the marginal capacity only to the low-availability node (i.e. *low-availability deployment range*). This is because marginal capacity allocated to the high-availability node would result in increasing marginal curtailment at the high-availability node, while small capacities at the low-availability node do not need to be curtailed. For even higher levels of VRE penetration, resulting in curtailment at the low-

availability node, it is optimal for producers to split marginal capacity between the two nodes (i.e. *split capacity deployment range*). Thus, at higher levels of VRE penetration, it is welfare-enhancing to allocate (some) VRE capacity to less favourable sites from the perspective of potential supply. The VRE penetration levels, which mark the cut-off points between the three ranges, I derive analytically. The results imply, that the cut-off points depend on the parameter configuration of the system topology.

Therefore, the system topology affects the width of the *high-* and *low-availability deployment range* and the capacity split under the *split capacity deployment range*. Increasing the transmission capacity and demand share at the high-availability node widens the *high-availability deployment range* and narrows the *low-availability deployment range*. In the *split capacity deployment range*, more capacity is allocated to the high-availability node. A higher correlation between the nodal availability profiles increases the share of capacity allocated to the high-availability node in the *split capacity deployment range*. Higher availabilities at the low-availability node narrow the *high-availability deployment range* so that the overall share of VRE allocated to the low-availability node increases. The impact of nodal availability profiles is found to be influenced by transmission capacity. In the case of correlation, the impact of changes in correlation increases with increasing transmission capacity. The direction of the effect of changes in the availability and variance in the *split capacity deployment range* even depends on the transmission capacity. Increasing the average and decreasing the variance of the nodal availability increases the nodal share when the transmission capacity is high. The opposite happens when the transmission capacity is low. Therefore, the availability profiles alone are not sufficient to indicate the optimal spatial allocation but need to be considered in combination with the level of transmission capacity.

Regarding the second research question, my analysis provides the following insights: Under uniform pricing, producers allocate capacity only to the high-availability node for higher VRE penetration levels than socially optimal. This is because network constraints that would induce producers to allocate capacity more in line with demand are ignored. Welfare losses occur when marginal curtailment due to limited transmission capacity exceeds the average availability advantage of the high-availability node. Welfare losses increase with increasing VRE penetration until VRE penetration is sufficiently high that differences in availability profiles provide an incentive to allocate some capacity to the low-availability node. Welfare losses under uniform pricing decrease with the level of transmission capacity and increase with the need for transmission.

From a theoretical perspective, my contribution is threefold: First, using a highly stylised model, I show that the optimal spatial allocation can be grouped into three ranges. I analytically derive the VRE penetration

levels that separate the three ranges, so that the results can be applied to any feasible configuration of the system topology. Second, I identify the effect of various parameters of the system topology on the optimal spatial allocation of the ranges. And third, I identify the allocation under uniform pricing and the resulting welfare loss, and show how the welfare loss is affected by the different parameters of the system topology. Due to my model's simplicity, I analyse a highly stylised setting. When analysing a more realistic setting additional effects will occur. Such effects from considering a more realistic setting on my theoretical findings are discussed in Chapter 5. Combining the findings from the theoretical analysis with the considerations from the discussion can help policymakers when designing policies that affect the spatial allocation or when considering a change in the market design. Investors can use the results when trying to find the profit-maximising allocation of VRE investments.

2. Model

I develop a theoretical model to analyse the effect of the VRE penetration, the transmission capacity, the demand distribution, the VRE availabilities, and the market design on the spatial allocation of VRE capacity. The effect of storage and demand flexibility I do not analyse in the model itself to ensure an analytical solution. To shed light on the effect of storage and demand flexibility, I discuss the effects qualitatively based on the model results and findings from other papers in Chapter 5.

The model considers the interaction between profit-maximising producers in a perfectly competitive environment, consumers, and a regulator. The players act in a network consisting of two nodes, h and l (i.e., $i \in (h, l)$), which are connected by a transmission line with the transmission capacity t. Furthermore, I define the model to have three stages, the regulation stage (τ_1), the spatial allocation stage (τ_2), and the market clearing stage (τ_3). As the model is solved by backward induction, the explanation starts with the last stage.

The market clearing stage (τ_3) takes place for a time interval ranging from 0 to 1. The time interval is divided into n periods with equal length, where n goes towards infinity ($n \to \infty$). I assume the consumers' demand at each node (d_i) is constant among all n periods, inelastic and exceeds the transmission capacity (i.e., $d_i > t$). I denote the demand in terms of power[1], such that the demand for a specific period r and the total demand in stage τ_3 coincide. Due to assuming a time interval ranging from 0 to 1, the demand in stage τ_3 in terms of energy[2] and power coincide as well (i.e., $\sum_{r=1}^{n} \frac{1}{n} d_i = d_i$).

[1] Demand denoted in terms of power defines the rate at which electricity is retrieved from an electrical network. A well known unit for power is Watt.

[2] Demand denoted in terms of energy defines the sum of electricity retrieved from an electrical network.

I assume that the producers can satisfy the demand with one conventional and one VRE technology. This assumption differs from the situation in most countries, where several conventional and at least two VRE technologies, namely wind and solar, are employed. On the one hand, the assumption of one conventional and one VRE technology allows me to derive the effect of the spatial allocation of VRE analytically. This provides a general understanding of the impact of the system topology. On the other hand, the simplification of multiple production technologies into one conventional and one VRE technology highlights the stylised nature of the model. The implications of this simplification are discussed in Chapter 5. The conventional technology induces constant marginal production costs. When supplying one unit throughout the time interval ranging from 0 to 1 the costs are equal to c.[3]. I assume the conventional capacity at nodes h and l to exceed the respective demand. As the producers operate in a competitive environment, they cannot charge prices above the marginal costs c of the conventional technology. Therefore, producers cannot make profits by investing in the conventional technology and have no incentive to invest in this technology.[4]

The VRE technology induces zero marginal costs. However, the capacity is limited to the total VRE capacity v (also denoted as VRE penetration). The capacity at nodes h and l is represented by V_h and $V_l = v - V_h$. The VRE capacity cannot always produce at full capacity, but only at the availability ($avail_{i,r}$) times the installed capacity (V_i). The availability varies between the nodes (denoted by the index i) and the periods (denoted by the index r). Within the time interval ranging from 0 to 1, I assume the availabilities to constantly change. The temporal sequence of all availabilities occurring during the interval I define as availability profile (i.e., $AVAIL_i$). I assume the availability profile to be a deterministic sequence which is characterised by an average (μ_i) and variance (σ_i^2). The values within the availability profile are assumed to be beta distributed. The beta distribution is chosen because it features positive densities only for values in the interval $[0, 1]$, as VRE availabilities do in reality.[5] Hence, the density function describing the distribution of the availabilities within the availability profile is given by:

$$f_{AVAIL_i} = \int_0^1 \frac{1}{B(\alpha_i, \beta_i)} x^{\alpha_i - 1}(1-x)^{\beta_i - 1} dx \tag{1}$$

Choosing the parameters α_i and β_i appropriately, results in density functions similar to the realised densities

[3]These costs include fuel costs as well as other all relevant variable costs such as costs for carbon emission allowances.

[4]In reality, investment in conventional capacity can be observed. There are two main reasons for this. First, conventional capacity often does not exceed demand, so producers can make profits by offering capacity in periods of scarcity. Such scarcity tends to persist as older plants are retired. Second, the marginal cost of building new conventional technologies tends to fall over time, so that new capacity can be profitable even in the absence of scarcity.

[5]In accordance with the Moivre-Laplace theorem, assuming n to converge towards infinity allows to represent the discrete binomial beta distribution by the continuous beta distribution.

of wind or solar power plants, as shown in Chapter Appendix B.

The potential supply in terms of power at node i and period r (denoted by $PS_{i,r}$) is given by the product of the respective availability and the installed capacity:

$$PS_{i,r} = V_i \cdot avail_{i,r} \tag{2}$$

The potential supply within the time interval ranging from 0 to 1 (both defined in terms of power and energy) is defined by:

$$PS_i = V_i \cdot \frac{1}{n} \sum_r avail_{i,r} \tag{3}$$

As the beta distribution describes the deterministic availability profile's distribution, the potential supply can be expressed as follows:

$$\begin{aligned} PS_i &= V_i \cdot f_{AVAIL_i} \\ PS_i &= V_i \int_0^1 \frac{1}{B(\alpha_i, \beta_i)} x^{\alpha_i - 1}(1-x)^{\beta_i - 1} dx \end{aligned} \tag{4}$$

By integrating Equation 4 and by considering $\mu_i = \frac{\alpha_i}{\alpha_i + \beta_i}$ the PS_i can be simplified as follows[6]:

$$PS_i = V_i \mu_i \tag{5}$$

I assume $\mu_h > \mu_l$, so that I call node h as *high-availability node* and node l as *low-availability node*. Further, I assume the joint distribution of nodal availability profiles to be deterministic as well. This implies, that the availabilities occurring jointly at the high- and low-availability node are known at any period (r) by the producers. The availabilities at the two nodes can be correlated, with $\rho_{h,l} \in (-1, 1)$ being the correlation coefficient. Highly correlated availabilities (i.e., $\rho_{h,l}$ close to 1) imply that a high availability in h tends to coincide with a high availability in l and vice versa. If the availabilities are barely correlated (i.e., $\rho_{h,l}$ close to 0), high availabilities in h are similarly likely to be accompanied by high or low availabilities in l. Independent of the correlation coefficient, I assume that within the sequence of n periods (with $n \to \infty$) there is a period with an availability equal to 1 at both nodes simultaneously (i.e., $avail_{h,r} = avail_{l,r} = 1$).

The potential VRE supply which can neither be consumed locally nor be exported is curtailed. The

[6]Next to mean the variance is defined by $\sigma_i^2 = \frac{\alpha_i \beta_i}{(\alpha_i + \beta_i + 1)(\alpha_i + \beta_i)^2}$. Both parameters, α and β, affect the average and the variance simultaneously. However, for $\mu_i \in [0.2, 0.4]$, increasing α_i primarily increases μ_i, while σ_i is barely affected. A numerical example showing these effects I provide in Chapter Appendix E.

curtailment I denote with K. The difference in global potential supply ($\sum_i PS_i$) and curtailment (K) I define as usable supply (US):

$$US = \sum_i PS_i - K \tag{6}$$

The curtailment (K) can be grouped into to types. First, curtailment can arise when limited transmission capacity prevents the export of potential supply to the neighbouring node (K_i^t). Second, curtailment can arise when the global potential supply excluding the curtailment from limited transmission capacity exceeds the global demand (K^d).

$$K = \sum_i K_i^t + K^d \tag{7}$$

In the spatial allocation stage (τ_2), the producers allocate the VRE capacity between nodes h and l. The respective capacities I define as V_h and $V_l = v - V_h$. I model the spatial allocation of all VRE capacity as a one-shot game where producers consider a particular system topology, i.e. transmission capacity, spatial distribution of demand, VRE penetration and VRE availability. This differs from reality, where VRE penetration increases continuously and other system topology parameters also evolve over time. The implications of assuming a one-shot game I discuss in Chapter 5.

Producers choose the allocation between h and l such that their profits are maximised. When deciding on the spatial allocation, the producers have perfect foresight, i.e., they know the nodal demand and the nodal availability profiles. In addition, producers take into account the underlying market design as well as the total level of VRE capacity. All parameters presented, namely the demand (d_i), the transmission capacity (t), the VRE penetration (v), and the parameters determining the nodal availability profiles (μ_i, σ_i, $\rho_{h,l}$) define the system topology.

In this paper, I focus on the optimal spatial allocation of VRE and not on the optimal capacity (v). Therefore, I assume that the regulator defines the total VRE capacity in the regulation stage (τ_1).[7, 8]

In addition, the regulator defines the market design. The market design options the regulator can implement are nodal and uniform pricing. Under nodal pricing the nodal demand and supply define the nodal price, considering the network transmission capacity. The prices at both nodes may differ, as shown in

[7] To identify the optimal v in the model at hand one would have to consider the capital costs of the VRE technology and minimise the total costs with respect to the total VRE capacity.

[8] When the regulator defines v, she may use auctions which allow for negative prices and contain an obligation to build the purchased capacity. Such a process would ensure the total capacity is sold in this stage, built and allocated in the spatial allocation stage and used in the market clearing stage.

the following example: Assume the potential VRE supply at node h at period r exceeds the nodal demand plus the transmission capacity ($PS_{h,r} > d_h + t$). In that case, some VRE at node h needs to be curtailed, and the VRE technology sets the nodal price. As the VRE technology features zero marginal costs the price at node h is zero (i.e., $p_{h,r} = 0$). At the same time, the potential VRE supply at node l plus the VRE imports from node h is below the demand in l (i.e., $PS_{l,r} < d_l - t$). As a result, some conventional supply is required to satisfy the demand at node l, such that the conventional technology sets the price (i.e., $p_{l,r} = c$). Depending on the system topology, the price at both nodes will be c in some periods and 0 in others. The proportion of periods where the conventional technology sets the price represents the average nodal price $\overline{p_i}$.

Under uniform pricing, the price producers receive is determined by the global demand ($d_h + d_l = d_{h+l}$) and global supply. Thus, the market design implicitly ignores transmission constraints and yields identical prices at both nodes (i.e., $p_{h,r} = p_{l,r}$). The conventional technology sets the price (i.e., $p_i = c$) when the global demand exceeds the global VRE potential. When the global VRE potential exceeds the global demand, the VRE technology sets the price (i.e., $p_{i,r} = 0$). The proportion of periods where the conventional technology sets the price represents the average price $\overline{p_i}$. Under uniform pricing, periods may arise where supply sold with VRE supply cannot be dispatched to the consumers due to limited transmission capacity. I assume such VRE supply is curtailed, but producers still receive the market price. This is similar to the compensation applied in multiple countries with uniform pricing, such as Germany, Denmark, Italy or Japan (Bird et al., 2016). To ensure demand is met, the curtailed VRE supply is replaced by an additional conventional supply at the other node. Such conventional supply I denote by redispatch. These costs are assumed to be borne by the consumers. Figure 1 schematically represents the model setup including the three stages.

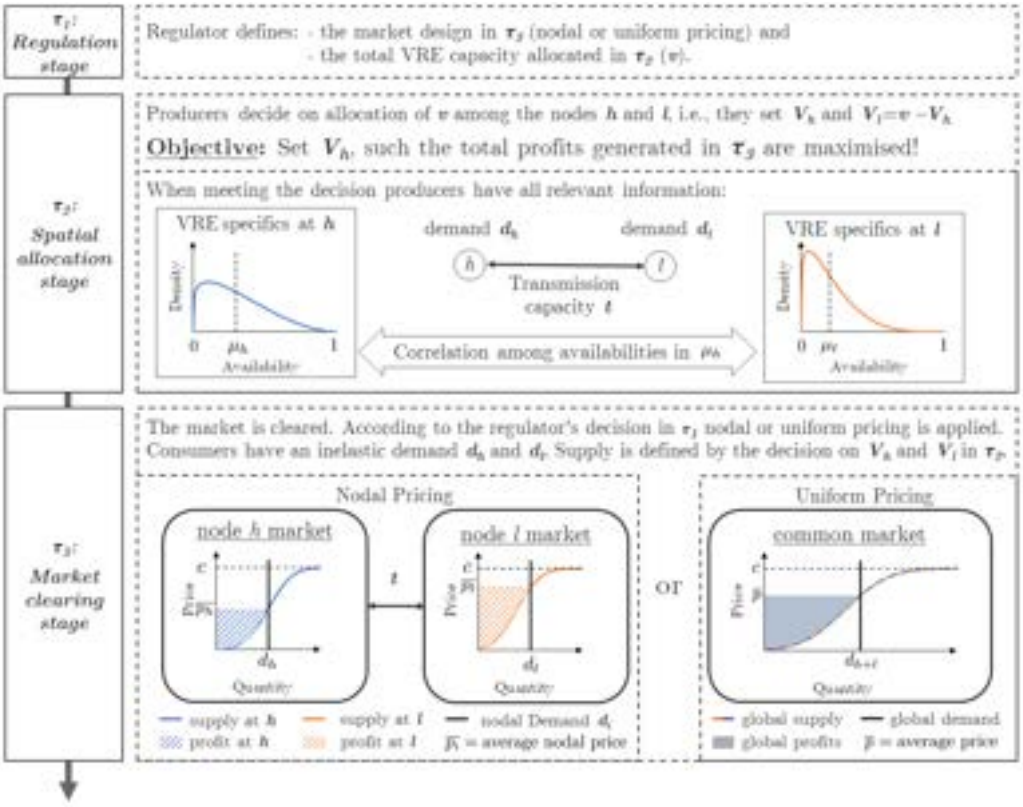

Figure 1: Schematic representation of the model setup.

3. Spatial allocation under nodal pricing

In this chapter, I analyse the socially optimal spatial allocation under nodal pricing. One crucial aspect influencing the spatial allocation is the occurrence and the level of curtailment at the high- and low availability node. This curtailment depends on the relative level of VRE penetration with respect to the other parameters, such as nodal demand or transmission capacity. In a first step, I identify three ranges of capacity allocation, valid for different relative levels of VRE penetration. In a second step, I assess the effect of transmission capacity, nodal demand distribution, and VRE availability profiles on the width of the ranges and spatial allocation within the ranges. Within the analysis, I consider the interactions among the parameters.

3.1. Capacity allocation ranges

In this subchapter, I derive the capacity allocation ranges under nodal pricing for different relative levels of VRE penetration. I conclude that:

Finding NP 1. *The optimal spatial allocation can be grouped into three spatial allocation ranges which are valid for different levels of VRE penetration. For low VRE penetration levels, producers allocate marginal*

capacity to the high-availability node (high-availability deployment range). For higher VRE penetration levels, producers allocate marginal capacity to the low-availability node (low-availability deployment range), and for even higher VRE penetration levels, producers split marginal capacity among the two nodes (split capacity deployment range).

Explanation. Under nodal pricing, perfect competition and perfect information, the producers' maximisation of profits coincides with the minimisation of the total costs (TC). Hence, producers spatially allocate the capacity such that the total costs are minimised. Within the total costs, the capacity level at node l (V_l) can be substituted with $v - V_h$, such that V_h is the only decision variable. The total costs are given by the conventional production times their marginal costs (c). The level of conventional production is given by the global demand (d_{h+l}) minus the usable supply (US) generated by VRE capacity. As the usable supply is defined by the difference between the global potential supply ($\sum_i PS_i$) and curtailment (K), the total costs are given by:

$$\min_{V_h} \; TC = \Bigg(d_{h+l} - \underbrace{\Big(\sum_i PS_i(V_h) - K(V_h) \Big)}_{\text{usable supply}} \Bigg) c \quad \text{for } V_h \in [0, v] \tag{8}$$

By substituting $PS_i(V_h)$ with the definition given in Equation 5 the objective function can be rewritten as follows:

$$\min_{V_h} \; TC = \Bigg(d_{h+l} - \underbrace{\Big(V_h \mu_h + (v - V_h)\mu_l - K(V_h) \Big)}_{\text{usable supply}} \Bigg) c \quad \text{for } V_h \in [0, v] \tag{9}$$

The global demand (d_{h+l}) is a constant and hence independent of V_h. Further, the cost parameter c is positive by definition. Hence, the total costs are minimised by maximising the level of usable supply (US).

Case 1: No curtailment

In the absence of curtailment the usable supply coincides with the potential supply. Hence the objective function is minimised by maximising the potential supply. Since $\mu_h > \mu_l$ by definition the total costs are minimised by allocating all capacity to node h.

Curtailment is absent if the installed capacity at node h does not exceed the nodal demand plus the transmission capacity (i.e., $v < d_h + t$), such that:

$$V_h^*(v) = v \quad \text{if: } v \leq d_h + t \tag{10}$$

Case 2: Curtailment at node h

When VRE penetration exceeds the nodal demand at the high-availability node plus the transmission capacity ($v > d_h + t$), increasing the capacity at node h induces curtailment (K). The curtailment in this case arises at node h due to limited transmission capacity (K_h^t). The existence of curtailment implies that the usable supply is smaller than the potential supply. The optimal allocation in this case depends on the level of curtailment. For VRE penetration levels represented in Case 2, marginal curtailment which only occurs at node h is strictly monotonically increasing in the VRE penetration, given that capacity is only allocated to node h (i.e. $V_h = v$).[9] Due to the strict monotonicity of marginal curtailment occurring at node h two sub cases arise:

Case 2a: Allocating capacity to node h

In Case 2a it is optimal to allocate all capacity at node h. This requires the marginal usable supply to be higher at node h than at node l when increasing the VRE penetration (v) marginally. Hence, in this case, a marginal increase in v evaluated at $V_h = v$ results in a marginal curtailment which is smaller than the delta in marginal potential supply between the high- and the low-availability node:

$$\left.\frac{\partial K}{\partial v}\right|_{V_h=v} \leq \mu_h - \mu_l \tag{11}$$

The strict monotony of curtailment in v, given $V_h = v$ implies that there is a VRE penetration level at which marginal curtailment reaches the delta in marginal potential supply between the high- and the low-availability nodes (i.e., $\left.\frac{\partial K}{\partial v}\right|_{V_h=v} = \mu_h - \mu_l$). Hence, the strict monotony of curtailment implies the existence of a cut-off point between Case 2a and Case 2b which I discuss below. The VRE penetration which induces $\left.\frac{\partial K}{\partial v}\right|_{V_h=v} = \mu_h - \mu_l$ marks the highest VRE penetration at which producers allocate all capacity to the high-availability node. The cut-off point I denote by:

$$v^{H|L} = v\left[\left.\frac{\partial K}{\partial v}\right|_{V_h=v} = \mu_h - \mu_l\right] \tag{12}$$

Case 2b: Allocating capacity to node l

When v exceeds $v^{H|L}$, it is no longer optimal to allocate all capacity to node h. For such higher level of v a marginal increase in VRE penetration evaluated at $V_h = v$ results in a marginal curtailment which is higher

[9] I derive the strict monotonicity mathematically in Appendix A.2.

than the delta in marginal potential supply between the high- and the low-availability node:

$$\left.\frac{\partial K}{\partial v}\right|_{V_h=v} > \mu_h - \mu_l \tag{13}$$

This implies the marginal usable supply when allocating a marginal capacity unit to node h is lower than the marginal potential supply at node l. At node l curtailment is absent for initial capacity allocations. Hence, marginal potential supply at node l coincides with marginal usable supply. Hence, for such VRE penetration levels it is optimal to allocate marginal capacity to node l.

As stated in Chapter 2, I assume that an availability of 1 occurs simultaneously at both nodes (i.e., $avail_{h,r} = avail_{l,r} = 1$). Further I know from Case 1 and 2a that $V_h \geq d_h + t$. Hence, when VRE penetration at node l reaches $d_l - t$, there is a period at which supply can fully serve the demand at node h and l.[10] Allocating further capacity to node l would yield to curtailment. Hence, $V_l = d_l - t$ marks the end of Case 2b. The overall VRE penetration at this cut-off point is given by:

$$v^{L|S} = v^{H|L} + (d_l - t) \tag{14}$$

Summarising the results of Case 2, results in the following optimal spatial allocation:

$$V_h^*(v) = \begin{cases} v & \text{if:} \quad d_h + t < v \leq v^{H|L} \\ v^{H|L} & \text{if:} \quad v^{H|L} < v \leq v^{L|S} \end{cases} \tag{15}$$

Case 3: Curtailment at both nodes

When VRE penetration exceeds $v^{L|S}$ curtailment occurs at both nodes. In addition to curtailment due to limited transmission capacity occurs (K_h^t), which occurs in Case 2, also curtailment due to global potential supply exceeding global demand (K^d) occurs in this case.[11]

At a penetration level of $v^{L|S}$, which marks the lower boundary of Case 3, the marginal curtailment at node h exactly compensates for the advantage in the nodal potential supply. As a result, the marginal usable supply at node h and l coincide. When adding marginal capacity, such that $v^{L|S}$ is exceeded, it can

[10] When both $avail_{h,r}$ and $avail_{l,r}$ are equal to 1, the VRE supply at node h can serve the nodal demand (d_h). Further VRE exports from node h to node l of t are feasible. The residual demand at node l, which is given by $d_l - t$ can be served by $V_l = d_l - t$.

[11] The level of K^d depends on the overall VRE capacity (v), the capacity allocation (V_i), the density of the nodal availability profiles (f_{AVAILL_i}), and the deterministic joint distribution of the nodal availability profiles. The joint availability distribution depends on the nodal beta distribution parameter α_i, β_i and the correlation $\rho_{h,l}$ among the nodal availability profiles and cannot be derived analytically. Hence, K^d cannot be derived analytically.

either be allocated to node h, to node l, or split among the nodes. When allocating the capacity to the high-availability node the nodal marginal usable supply would decrease as marginal curtailment increase. First, marginal curtailment due to limited transmission capacity would increase as such curtailment is strictly monotonically increasing in nodal VRE penetration (see Appendix A.2). Second, curtailment due to global supply exceeding global demand would start to occur. Allocating the capacity to the low-availability node would also decrease the nodal marginal usable supply as curtailment due to global supply exceeding global demand would start to occur. Hence, in order to achieve an marginal usable supply which coincides at both nodes, marginal capacities have to be split among the two nodes.

When splitting of capacity is optimal, the first-order condition is fulfilled:

$$\frac{\partial TC}{\partial V_h} = -\left(\mu_h - \mu_l - \frac{\partial K}{\partial V_h}\right)c = 0 \tag{16}$$

The optimal spatial allocation is then given by:

$$V_h^*(v) = V_h[\frac{\partial TC}{\partial V_h} = 0] \quad \text{if: } v > v^{L|S} \tag{17}$$

For relatively low VRE penetration levels within Case 3, the majority of the marginal capacity should be allocated to node l. This is because for $V_l \in (d_l - t, d_l + t)$ curtailment at node l only occurs when global supply exceeds global demand, while curtailment due to limited transmission capacity remains absent. With increasing v, the capacity at the low-availability node (V_l) eventually exceeds $d_l + t$, also inducing curtailment due to limited transmission capacity at node l. For such level of VRE penetration capacity should be split more equally among the two nodes.

Defining the capacity allocation ranges

Based on the results from the case analysis the ranges arise:

$$V_h^*(v) = \begin{cases} v & \text{if: } v \leq v^{H|L} \\ v^{H|L} & \text{if: } v^{H|L} < v \leq v^{L|S} \\ V_h[\frac{\partial TC}{\partial V_h} = 0] & \text{if: } v > v^{L|S} \end{cases} \tag{18}$$

For relatively low VRE penetration ($v < v^{H|L}$) capacity is allocated only to the high-availability node. I denote this range as *high-availability deployment range*. For higher VRE penetration levels ($v^{H|L} < v \leq v^{L|S}$),

producers allocate capacity to the low-availability node. I denote this range as *low-availability deployment range*. For even higher VRE penetration levels ($v > v^{L|S}$), producers split the capacity among the two nodes. This range I denote as *split capacity deployment range*.

End of Explanation.

Figure 2 demonstrates the insights from Finding NP 1 numerically. The optimisation problem solved numerically to generate this and the remaining figures in this chapter resembles the optimisation problem described in Chapter 2 and solved in this chapter. Differences in the formulation arising from using a numerical instead of an analytical approach are described in Appendix D. The availability density parameters are chosen to resemble the availabilities for wind in the north (h) and south (l) of Germany. A comparison of the assumed and the historical German availability density for wind power is presented in Appendix C. The demand is split equally among the nodes, and the transmission capacity can transmit one-fourth of the nodal demand. The orange line in the upper diagram displays the marginal capacity share allocated to node h. A value of 1 indicates that producers allocate marginal capacity units to node h, while 0 indicates the marginal capacity unit is allocated to node l. Values in between imply that producers split marginal capacity among the two nodes.

For low levels of VRE penetration, all capacity is allocated to node h (i.e., *high-availability deployment range*). For $v < d_h + t$ curtailment is absent. For $v = d_h + t$, VRE supplies roughly 20% of the demand. For higher VRE capacity levels, marginal curtailment is higher such that the marginally usable supply is lower. For $V^h = v^{H|L} = 1.1 d_{h+l}$, the marginal usable supply is identical at both nodes, and the *high-availability deployment range* ends. At this point, VRE supplies 33% of the demand.

When the global VRE share ranges between 33-40%, capacity is allocated solely to node l. The VRE penetration marking the shift from the *low-availability deployment range* to the *split capacity deployment range* is given by $v^{L|S} = 1.1 d_{h+l} + (d_l - h)$. At this VRE penetration level $V_l = d_l - l$ holds. For higher VRE shares, the capacity is split among the nodes. For low levels of VRE penetration within the *split capacity deployment range* (40-45% global VRE share) the majority of marginal capacity is allocated to node l . When VRE share rises above 45%, producers allocate roughly half of the capacity to each node.

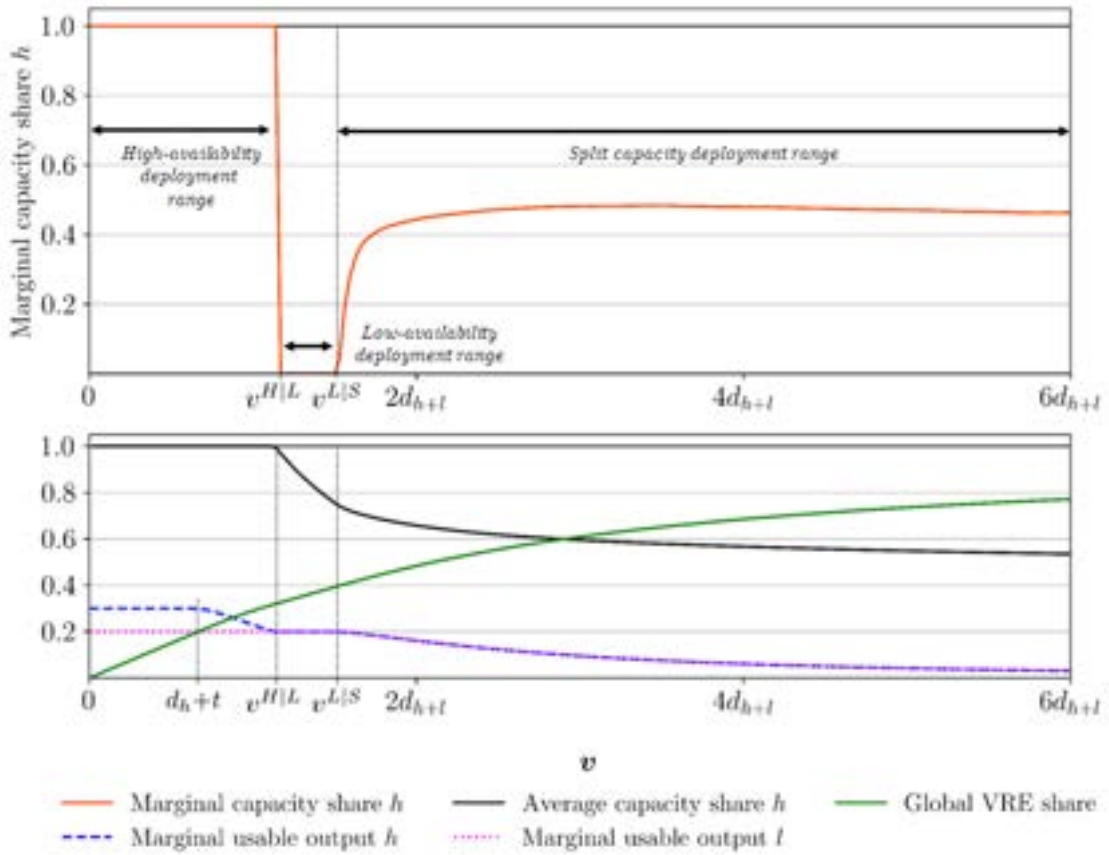

Parameter values: d_i=50, t=$\frac{1}{4}d_i$, $B_h(1.071, 2.5)\rightarrow\mu_h$=0.3, σ_h=0.21, $B_l(0.625, 2.5)\rightarrow\mu_l$=0.2, σ_l=0.20, $\rho_{h,l}$=0.6.

X-axis values: $v^{H|L} = 1.1d_{h+l}$ and $v^{L|S} = 1.1d_{h+l} + (d_l - t)$.

Figure 2: Spatial allocation, marginal usable supply, and VRE share at different VRE penetration levels under nodal pricing.

Additionally, the figure highlights the relevance of curtailment with increasing VRE penetration. At $v = 6d_{h+l}$, the potential supply exceeds 1.5 times the global demand. However, the VRE share remains below 80%. This is because roughly 50% of VRE supply is curtailed (not shown in the figure). The marginal curtailment at such a high VRE penetration level even reaches 85% at node l and 90% at node h (not shown in the figure).

Based on these observations, the question arises of how the transmission capacity, demand distribution, and availability profiles affect the capacity allocation ranges.

3.2. Effect of changes in the transmission capacity

In this subchapter, I derive the effect of changes in the transmission capacity (t) on the width of the capacity allocation ranges and the capacity split in the *split capacity deployment range*. Thereby the assumption $t < d_i$ (stated in Chapter 2) is relaxed. Based on the analysis, I conclude:

Finding NP 2. *Under nodal pricing, increasing the transmission capacity t widens the high-availability deployment range and narrows the low-availability deployment range. For $t \geq d_l$, the low-availability deployment range disappears. In the split capacity deployment range, the share of the high-availability node increases with increasing t.*

Explanation. Increasing the transmission capacity widens the *high-availability deployment range* as producers are willing to allocate capacity solely to the high-availability node for higher VRE penetration levels. This arises due to two effects: First, when increasing t by one unit, it is possible to add one unit of capacity at node h without inducing curtailment (refers to Case 1 of Finding NP 1).

Second, for v valid in Case 2 of Finding NP 1, marginal curtailment increase at a lower rate with increasing t.[12] The lower increase in marginal curtailment implies that the marginal usable supply is reduced at a lower rate. As a result the cut-off point between the *high-* and *low-availability deployment range* ($v^{H|L}$) is reached for higher levels of v. As both parts of the *high-availability deployment range* are widened, the range is widened as a whole.

With increasing the transmission capacity, the *low-availability deployment range* is narrowed. This is because the width of the range is given by $v^{H|L} - v^{L|S} = d_l - t$. For $t \geq d_l$, the *low-availability deployment range* disappears because supply produced at node h can serve the entire demand at node l. As a result, curtailment at node l already occurs for initial capacities. Hence, there is no VRE penetration level when producers are incentivised to allocate additional VRE units solely to node l.

In the *split capacity deployment range*, producers increasingly allocate capacity to the high-availability node when transmission capacity increases. This is because, with increasing t, network restrictions get less relevant, such that producers can increasingly exploit the more favourable VRE conditions at node h.

End of Explanation.

Figure 3 demonstrates the insights from Finding NP 2 numerically. The numerical example displays the marginal allocation share at node h and the marginal usable supply. Assumptions regarding the nodal demand (d_i), the availabilities ($B(\alpha_i, \beta_i)$) and the correlation among the availabilities ($\rho_{h,l}$) are identical to Figure 2.

First, marginal usable supply is constant for $V_h \leq d_h + t$, such that the first part of the *high-availability deployment range* gets wider with increasing t. Second, the increase in marginal curtailment (i.e., the

[12] I show this effect mathematically in Appendix A.3.1.

reduction in marginal usable supply) is dampened with increasing t. Hence, the second part of *high-availability deployment range* gets wider. While for $t = \frac{1}{4}d_i$ the width the range is roughly $1.1d_i$, it is 50% wider for $t = \frac{3}{4}d_i$.

When transmission capacity exceeds the nodal demand ($t \geq d_i$), only differences in production patterns (arising when $\rho_{h,l} < 1$) incentivise the allocation of capacity to node l. For the given numerical example, this is relevant only when the $v > 5d_{h+l}$.

Figure 3 also shows the shorting of the *low-availability deployment range*. While for $t = \frac{1}{4}d_i$ the range has a width of $\frac{4}{5}d_l$, the *low-availability deployment range* is narrowed to $\frac{1}{4}d_l$ if $t = \frac{3}{4}d_l$, and disappears if $t \geq d_l$.

Lastly, the figure shows the shift towards the high-availability node in the *split capacity deployment range*. While for $t = \frac{1}{4}d_i$ roughly 50% of marginal capacity is placed to node h when $v = 4d_{h+l}$, the nodal marginal capacity share at node h increases to 70% for $t = \frac{3}{4}d_i$.

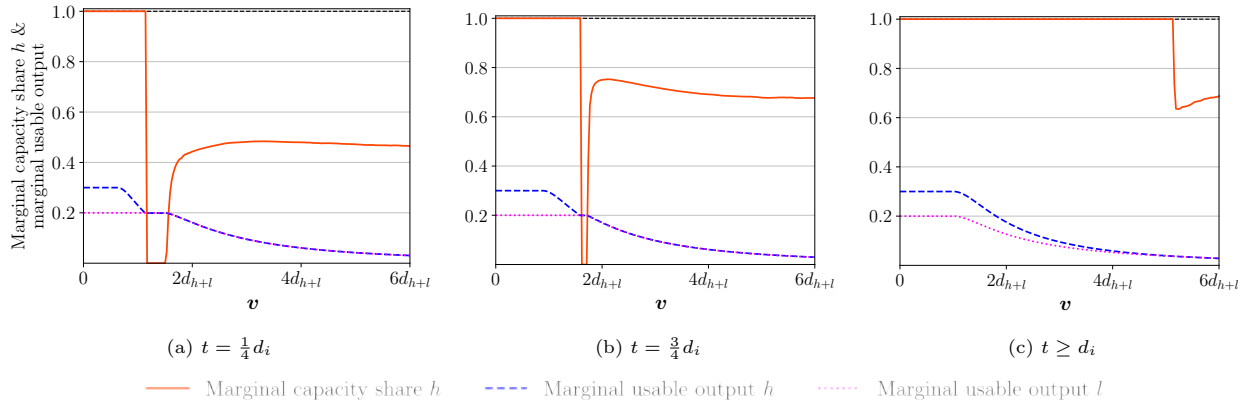

Figure 3: Effect of changes in the transmission capacity (t) on the spatial allocation ranges under nodal pricing.

3.3. Effect of changes in the demand distribution

In this subchapter, I derive the effect of the demand distribution on the capacity allocation ranges. Based on the analysis, I conclude:

Finding NP 3. *Under nodal pricing, increasing the demand at the high-availability node d_h widens the high-availability deployment range, while increasing d_l widens the low-availability deployment range. In the split capacity deployment range, the nodal share increases with the nodal demand.*

Explanation. Increasing the demand at node h widens the *high-availability deployment range*. This implies producers are willing to allocate capacity solely to the high-availability node for higher VRE penetration levels. This has two reasons: First, when increasing d_h by one unit, it is possible to add one unit of capacity

at node h without inducing curtailment (refers to Case 1 of Finding NP 1). Second, for v valid in Case 2 of Finding NP 1, the marginal curtailment increases at a lower rate with increasing d_h. As a result the cut-off point between the high- and low-availability deployment range ($v^{H|L}$) is reached for higher levels of v.[13]

With increasing d_l the *low-availability deployment range* is widened. This is because the width of the range is defined by $V_l > d_l - t$.

In the *split capacity deployment range*, increases in nodal demand motivate producers to increase the share of capacity they allocate to the node. This is because the more nodal demand and nodal supply are aligned, the lower the need for transmission and the lower the resulting curtailment from limited transmission capacity. Hence, when the demand increases at one node, curtailment can be reduced by shifting capacity to that node. The reduction in curtailment implies increased usable supply from VRE and decreased need for costly conventional power.

End of Explanation.

Figure 4 demonstrates the insights from Finding NP 3 numerically. Assumptions regarding the transmission capacity and the availability profiles are identical to Figure 2. When demand is mainly allocated to node l (i.e., $d_h = 25$ & $d_l = 75$), the *high-availability deployment range* is 5% smaller than the *low-availability deployment range*. Shifting demand from node l to node h widens the *high-availability deployment range* and narrows the *low-availability deployment range*. When demand is mainly allocated at node h (i.e., $d_h = 75$ & $d_l = 25$), the *high-availability deployment range* is 12 times as long as the *low-availability deployment range*. In the *split capacity deployment range*, the capacity share at node h increases from roughly 25% to 75% when shifting 50% of global demand from node l to node h.

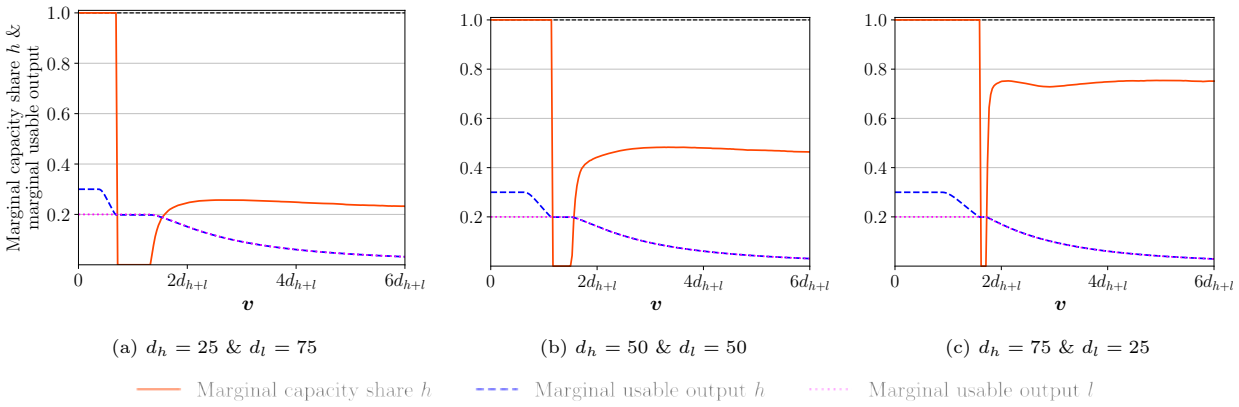

Figure 4: Effect of changes in the demand distribution on the spatial allocation ranges under nodal pricing.

[13] I show this effect mathematically in Appendix A.3.2.

3.4. Effect of changes in the availability profiles

In this subchapter, I derive the effects arising from different features of the availability profiles on the capacity allocation ranges under nodal pricing. To do so, I analyse the effects of changes in the correlation among nodal availability profiles and changes in the average and the variance of nodal availability profiles.

3.4.1. Correlation

In this subchapter, I derive the effect of the correlation among availability profiles on the capacity allocation ranges. Based on the analysis, I conclude:

Finding NP 4. *Under nodal pricing, changing the correlation among availability profiles $\rho_{h,l}$ does not affect the width of the high and low-availability deployment range. In the split capacity deployment range, increasing $\rho_{h,l}$ increases the capacity share allocated to the high-availability node. The effect increases with increasing t.*

Explanation. Under nodal pricing, changing the correlation among availability profiles $\rho_{h,l}$ does not affect the width of the *high-availability deployment range* because $\rho_{h,l}$ does not affect the nodal curtailment at node h when capacity at node l is absent (refers to Case 1 and 2a of Finding NP 1). Changing the correlation does also not affect the width of the *low-availability deployment range*. This is because the width of the range is defined by $d_l - t$ as shown in Finding NP 1 in Case 2b. The correlation between availabilities does not affect the producers' allocation decision as long as VRE penetration is sufficiently low, so curtailment at node l is absent.

In the *split capacity deployment range* when $K^d > 0$ the joint distribution of the availabilities affects the spatial allocation of VRE (refers to Case 3 of Finding NP 1). Increasing correlation shifts capacity towards the *high-availability node*. This is because the incentive for producers to allocate capacity to node l, namely exploiting the differences in availability profiles, is weakened with increasing correlation.

The extent of the effect increases with increasing transmission capacity (t). This is because, for low levels of t, the optimal allocation is mainly driven by the network restrictions. Producers reduce curtailment arising from limited transmission capacity to an appropriate level by allocating capacity relatively even among the nodes (see Finding NP 2). In such a case, the effect of correlation on the allocation is limited. Network restrictions are less relevant for high levels of t, and the availability profiles, including the differences in availability profile patterns, mainly drive the optimal allocation. Hence, the relevance of correlation on the producer's allocation decision in the *split capacity deployment range* increases with increasing t.

End of Explanation.

Figure 5 demonstrates the insights from Finding NP 4 numerically. Assumptions regarding the demand and the availability profiles are identical to Figure 2. The correlation varies in the interval 0 and 1 (i.e., $\rho_{h,l} \in [0, 1]$) for the case of low and high transmission capacity (i.e., $t = \frac{1}{4}d_i$ and $t = \frac{3}{4}d_i$).

Independent of the transmission capacity, the width of the *high* and *low-availability deployment range* are not affected by changes in the correlation.

In the *split capacity deployment range*, increasing $\rho_{h,l}$ increases the capacity share of the high-availability node. Analysing the nodal marginal capacity shares at $v = 6d_{h+l}$ shows that the effect of correlation on node-h-capacity-share increases with increasing transmission capacity. For low levels of transmission capacity (i.e., $t = \frac{1}{4}d_i$), the node-h-capacity-share increases by only 10% from 43% to 53% when $\rho_{h,l}$ is increased from 0 (uncorrelated) to 1 (perfectly correlated). When transmission capacity is high (i.e., $t = \frac{3}{4}d_i$), the node-h-capacity-share increases by almost 30% (i.e., from 55% to 83%) when $\rho_{h,l}$ is increased from 0 to 1.

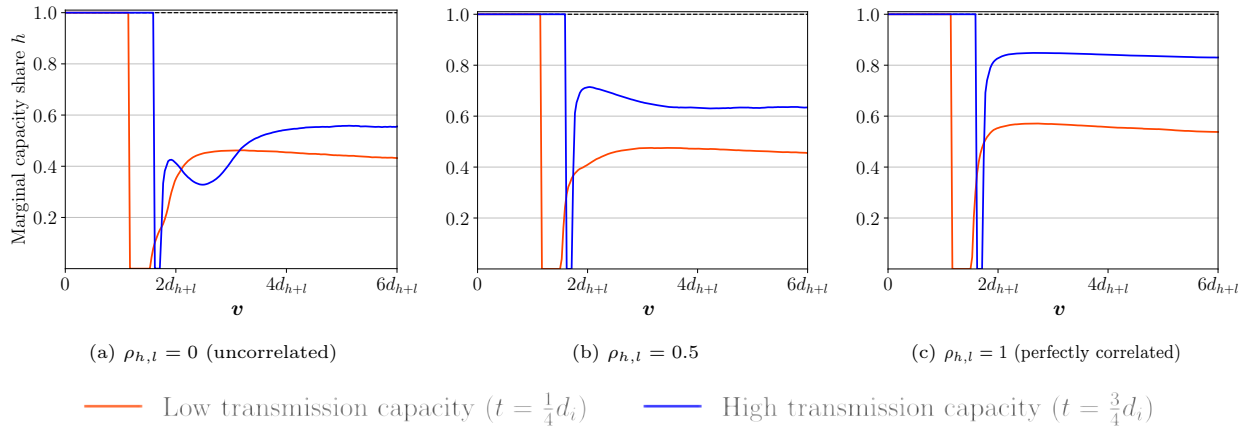

(a) $\rho_{h,l} = 0$ (uncorrelated) (b) $\rho_{h,l} = 0.5$ (c) $\rho_{h,l} = 1$ (perfectly correlated)

Figure 5: Effect of the correlation among availability profiles on the spatial allocation ranges under nodal pricing.

3.4.2. Average

In this subchapter, I derive the effect of the average availability on the capacity allocation ranges. The density of availabilities is described by the parameters α_i and β_i. As stated in Chapter 2, increasing α_i primarily increases the average availability, while the variance remains rather constant. To assess the effect of changes in the average availability, I analyse the effects arising from changes in α_i.[14] Based on the analysis, I conclude:

Finding NP 5. *Under nodal pricing, increasing the average availability μ_l by increasing α_l narrows the high-availability deployment range. The effect of μ_h on the high-availability deployment range and the effect of μ_i on the split capacity deployment range is ambiguous and depends on the system topology.*

[14] Changing μ_i while keeping the variance fully constant, i.e. also altering β_i, does not alter the findings. However, such an approach does not allow for analysing the effects analytically.

Explanation. With increasing average availability at node l the *high-availability deployment range* is narrowed, because the difference in the average availability between the high- and the low availability node is reduced. As a result, producers only tolerate lower marginal curtailment levels at node h when allocating capacity to the node (refers to Case 2a of Finding NP 1). This implies a narrowing of the *high-availability deployment range*.

Increasing the average availability at node h can either narrow or widen the *high-availability deployment range*. This is due to two opposing effects which occur for v valid in Case 2a of Finding NP 1: On the one hand, an increase in the average availability at node h increases the difference between the average availability at node h and h. This effect allows for higher curtailment at node h and incentives producers to widen the sole capacity allocation to node h. On the other hand, increases in nodal availability increase the marginal curtailment arising from limited transmission capacity. The increased relevance of network restrictions and the resulting increase in marginal curtailment incentive producers to narrow the sole capacity allocation to node h. Subtracting both effects yields the effect on the marginal usable supply. Depending on the parameters t, d_i, and $\beta_i(\alpha_i, \beta_i)$ as well as the nodal VRE capacity, V_i, the effect on marginal usable supply can either be positive or negative.[15] When t is low, the term tends to be negative in the relevant domain. Hence, when network restrictions are tight, the increase in marginal curtailment due to limited transmission capacity outweighs the increase in marginal potential supply. In such a situation, producers reduce the amount of capacity they solely allocate to node h, with increasing μ_h. When t is high, the term tends to be positive in the relevant domain. Hence, with increasing μ_h, producers increase the capacity they solely allocate to node h.

The width of the *low-availability deployment range* is given by $d_l - t$, such that it is not affected by μ_i (refers to Case 2a of Finding NP 1).

The effect of increasing average availability on the *split capacity deployment range* is ambiguous. This is also due to the two opposing effects of increased potential supply and curtailment. While producers tend to increase the nodal with increasing μ_i when t is high, the opposite is true for low levels of t.

End of Explanation.

Figure 6 displays the effects of changes in the average nodal availability on the capacity allocation in a numerical example. Assumptions regarding the demand, q_i, and the correlation are identical to Figure 2. To analyse the effect for low and high levels of transmission capacity, the marginal capacity shares are calculated for $t = \frac{1}{10}d_i = 5$ and $t = \frac{3}{4}d_i = 37.5$.

[15] I mathematically derive the effect of changes in α_h on the marginal usable supply in Appendix A.3.3.

When increasing μ_l from 0.2 to 0.25, the *high-availability deployment range* narrows by roughly 17% for both cases of transmission capacity (compare Figure 6a and c). All other effects when changing μ_i highly depend on the level of transmission capacity. In the numerical example, this can be observed best for the *split capacity deployment range*. When transmission capacity is low, a higher μ_h decreases the share of capacity allocated to node h by roughly 10-15 percentage points and increasing μ_l decreases the share of capacity allocated to node l by roughly 10-20 percentage points. When transmission capacity is high, the opposite effects occur. Higher μ_h increases the share of capacity allocated to node h by roughly five percentage points. Higher μ_l decreases the share of capacity allocated to node l by roughly 10-20 percentage points.

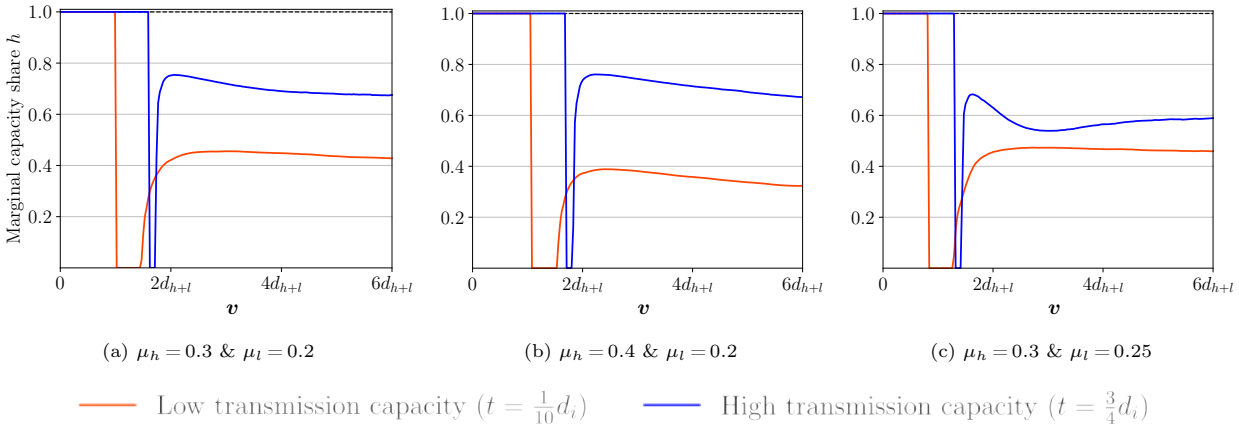

Figure 6: Effect of the average in the availability profile on the spatial allocation ranges under nodal pricing.

3.4.3. Variance

In this subchapter, I derive the effect of the variance in availability profiles (σ_i^2) on the capacity allocation ranges. The variance is defined by the availabilities density function, i.e., $B(\alpha_i, \beta_i)$. To analyse the effect of σ_i^2, the parameter values α_i and β_i are changed such that the average supply potential μ_i remains constant. Based on the analysis, I conclude:

Finding NP 6. *Under nodal pricing, higher variance at the high-availability node σ_h^2 narrows the high-availability deployment range. The effect of increases in the nodal variance on the split capacity deployment range is twofold: The nodal share decreases for moderate VRE penetration or high transmission capacity, while the nodal share increases when VRE penetration is high, and transmission capacity is low.*

Explanation. Under nodal pricing higher σ_h^2 narrows the *high-availability deployment range* due to higher marginal curtailment at node h. The increase in marginal curtailment results in the fact that Case 2a in Finding NP 1 is valid only for lower level of v. This can be explained as follows: The volatile potential supply

decreasingly matches the constant demand, such that the potential supply at node h more often exceeds $d_h + t$ requiring curtailment. As marginal curtailment is higher the usable supply at node h is equal to the potential supply at node l for lower levels of v.

The width of the *low-availability deployment range* is given by $d_l - t$, such that it is not affected by σ_i^2 (refers to Case 2b of Finding NP 1). The effect of increases in variance on the *split capacity deployment range* is twofold: On the one hand, increases in the variance reduce the overall usable supply as the potential supply decreasingly matches the nodal demand. As a result, increasing the variance reduces the marginal usable supply for low and moderate levels of VRE penetration. Producers are incentivised to allocate less VRE to the node with increased variance. On the other hand, increasing the nodal variance can increase the marginal usable supply for high levels of VRE penetration. This is because increases in the nodal variance lower the nodal VRE share. When nodal VRE shares are high (e.g. close to 100%), additional VRE can be barely used to serve the nodal demand. With lower VRE shares, due to increases in the variance, a higher share of the additional VRE can be used to serve the nodal demand and thereby increase the marginal usable supply. Hence, producers are incentivised to allocate more VRE to the node with increased variance when VRE penetration is high. The higher the VRE penetration, the stronger the effect. The effect gets weaker with increasing transmission capacity because VRE supply can be increasingly integrated by exports and high nodal VRE shares get less relevant.

End of Explanation.

Figure 7 displays the insights from Finding NP 6 numerically for the case of low transmission capacity (i.e., $t = \frac{1}{10} d_i$).[16] Assumptions regarding the demand, the average availability, and the correlation are identical to Figure 2. When the variance is increased at node h (compare Figure 7a and b), the *high-availability deployment range* is narrowed from $1.3d_{h+l}$ to $0.9d_{h+l}$. Additionally, the figure confirms that the effect on the *split capacity deployment range* is twofold. In the case of moderate VRE penetration levels (i.e., roughly $v \leq 4d_{h+l}$), increasing σ_h^2 lowers the share of capacity allocated to node h. Such changes occur for VRE shares below 70%, as indicated by the green line. For high VRE penetration levels (i.e., $v \leq 4d_{h+l}$ or a VRE share above 70%), increasing σ_h^2 increases the share of capacity allocated to node h. Comparing the green lines also illustrates the decrease in the global VRE share. When the variance is increased at node l (compare Figure 7a and c)), the *high-availability deployment range* is not affected. The effect on the *split capacity deployment range* is the same as in the case of increases in σ_h^2. For moderate VRE penetration levels, higher

[16] A numerical analysis for the case of high transmission capacity is shown in Chapter Appendix F.

σ_l^2 lower the share of capacity allocated to node l (i.e., more capacity is allocated to node h). For high VRE penetration levels, higher σ_l^2 increase the share of capacity allocated to node l.

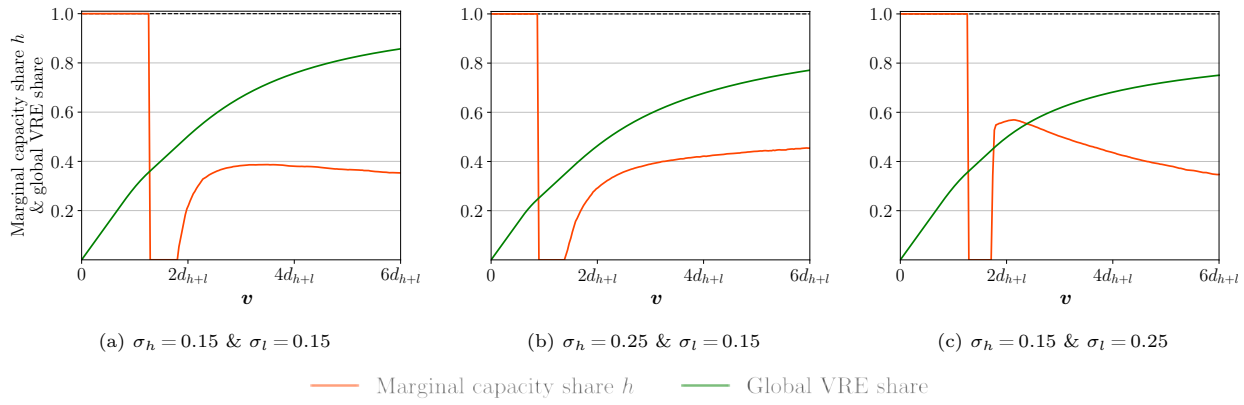

(a) $\sigma_h = 0.15$ & $\sigma_l = 0.15$ (b) $\sigma_h = 0.25$ & $\sigma_l = 0.15$ (c) $\sigma_h = 0.15$ & $\sigma_l = 0.25$

Figure 7: Effect of the variance in the availability profile on the spatial allocation ranges under nodal pricing.

4. Spatial allocation under uniform pricing

In this chapter, I analyse the spatial allocation under uniform pricing. The structure is similar to the previous chapter. First, I identify the two ranges of capacity allocation, valid for different relative levels of VRE penetration. Within the analysis, I assess the inefficiency by comparing the results to the optimal spatial allocation I derived in Chapter 3. Second, I analyse how various parameters of the system topology, namely the transmission capacity, the demand distribution, and the characteristics of the VRE availability profile, drive the spatial allocation and the resulting inefficiencies. Within the analysis, I assess the interactions among the parameters.

4.1. Capacity allocation ranges

In this subchapter, I derive the capacity allocation ranges under uniform pricing for different relative levels of VRE penetration. I conclude that:

Finding UP 1. *Under uniform pricing, the spatial VRE allocation encompasses the high-availability deployment range and the split capacity deployment range. Allocation is efficient when VRE penetration is low. With increasing VRE penetration inefficiencies emerge. These resulting welfare losses increase until marginal capacity is split among nodes.*

Explanation. Uniform pricing implicitly ignores network constraints when deriving market prices. Hence, the producers' profit maximisation problem coincides with minimising the total costs when ignoring network

constraints, denoted by DTC. DTC is given by the global supply of the conventional technology before redispatch times the marginal costs of the conventional technology (c). The global supply of the conventional technology before redispatch arises from the global demand minus the global supply of the VRE technology sold to the market. This supply I also denote as saleable supply (SS). The saleable supply is given by the global potential supply minus the supply, which cannot be sold to the market (i.e., $SS = \sum_i PS_i - \overline{K^c}$). The supply which cannot be sold to the market is denoted as commercial curtailment ($\overline{K^c}$). Hence, the objective function for the case of uniform pricing is given by:

$$\min_{V_h} \; DTC = \Bigg(d_{h+l} - \underbrace{\Big(V_h \mu_h + (v - V_h)\mu_l - \overline{K^c}(V_h) \Big)}_{\text{saleable supply}} \Bigg) c \quad \text{for } V_h \in [0, v] \tag{19}$$

The global demand (d_{h+l}) is a constant and hence independent of V_h. Further, the cost parameter c is positive by definition. Hence, the distorted total costs are minimised by maximising the level of saleable supply (SS).

Case 1: No commercial curtailment

In the absence of commercial curtailment the saleable supply coincides with the potential supply. Hence the objective function is minimised by maximising the potential supply. Since $\mu_h > \mu_l$ by definition the total costs are minimised by allocating all capacity to node h.

Supply is commercially curtailed when the global supply exceeds the global demand. As stated in Chapter 2, I assume that there is a period r with an availability equal to 1 at both nodes simultaneously (i.e., $avail_{h,r} = avail_{l,r} = 1$). Hence, commercial curtailment is absent if the installed capacity does not exceed the global demand:

$$V_h^{UP*}(v) = v \qquad \text{if: } v \leq d_{h+l} \tag{20}$$

Case 2: Presence of commercial curtailment

When VRE penetration exceeds the global demand ($v > d_{h+l}$), increasing the capacity at either node induces commercial curtailment ($\overline{K^c}$). This implies that the saleable supply is smaller than the potential supply. The optimal allocation of marginal capacity in this case depends on the level of marginal commercial curtailment. This results in two sub cases:

Case 2a: Allocating capacity to node h

In Case 2a it is optimal to allocate all capacity to node h. This requires the marginal saleable supply to be higher at node h than at node l when increasing the VRE penetration (v) marginally. Hence, a marginal

increase in v, evaluated at $V_h = v$, yields in a marginal commercial curtailment which is smaller than the delta in marginal potential supply between the high- and the low-availability node minus the marginal curtailment that would happen when placing the marginal capacity at node l.

For which level of v this is the case cannot be derived analytically, as I cannot derive $\overline{K^c}$ analytically.[17] However, I can explain the general rationale present in Case 2a. Later a numerical example will confirm the explanation:

At $v = d_{h+l}$ commercial curtailment is zero, i.e., there is no period in which $\sum_i PS_{i,r} > d_{h+l}$. When adding marginal capacity at node h such that d_{h+l} is exceeded commercial curtailment occurs. The commercial curtailment induced by the marginal capacity allocated to node h is very low for v, only slightly exceeding d_{h+l}. This is because $\overline{K_r^c}$ is positive only in those periods r with an $avail_{h,r}$ close to 1.

The marginal saleable supply decreases faster at node h than at node l, when the availability profiles are not perfectly correlated $\rho_{h,l} < 1$. This is because VRE production follows the availability profile of node h. When allocating additional capacity to node h the high additional potential supply at node h occurs in periods with commercial curtailment. When allocating additional capacity to node l and nodal availability profile patterns differ, the periods with potential supply at node l less often occur in periods with commercial curtailment. The VRE penetration v, which induces the marginal supply to coincide between the high- and low availability node, marks the cut-off point ($v^{UP/H|S}$). On this occasion, the first-order condition is fulfilled for $V_h = v$:

$$\left.\frac{\partial DTC}{\partial V_h}\right|_{V_h=v} = -\left(\mu_h - \mu_l - \left.\frac{\partial \overline{K^c}}{\partial V_h}\right|_{V_h=v}\right)c = 0 \tag{21}$$

Hence, the cut-off point can be expressed as follows:

$$v^{UP/H|S} = v[\left.\frac{\partial DTC}{\partial V_h}\right|_{V_h=v} = 0] \tag{22}$$

Case 2b: Splitting capacity among node h and l

For $v > v^{UP/H|S}$ profit maximising producers split the capacity among the high- and low-availability node. This can be explained as follows: At $v = v^{UP/H|S}$ the marginal saleable supply is identical at the high- and low availability node. When adding one unit of capacity, such that $v^{UP/H|S}$ is exceeded, it can either be allocated to node h, to node l or split among the nodes. In line with the explanation given in Case 2a, adding

[17] The level of $\overline{K^c}$ depends on the overall VRE capacity (v), the capacity allocation (V_i), the density of the nodal availability profiles (f_{AVAILi}), and the deterministic joint distribution of the nodal availability profiles. The joint availability distribution depends on the nodal beta distribution parameter α_i, β_i and the correlation $\rho_{h,l}$ among the nodal availability profiles, which cannot be derived analytically.

VRE capacity solely to node h would result in marginal saleable supply of node h to drop below the one of node l. Hence, producers will not allocate the additional capacity solely to node h. However, adding the VRE capacity solely to node l would result in marginal saleable supply at node l dropping below the one at node h. This is because also in when allocating capacity to node l commercial curtailment would increase. Hence, profit maximising producers split the capacity among the high- and low-availability node, such that the marginal saleable supply is identical at the high- and low-availability node.

When the splitting of capacity results in a profit maximising allocation the first-order condition is fulfilled:

$$\frac{\partial DTC}{\partial V_h} = -\left(\mu_h - \mu_l - \frac{\partial \overline{K^c}}{\partial V_h}\right)c = 0 \tag{23}$$

Summarising the results of Case 2 yields in the following profit maximising spatial allocation under uniform pricing:

$$V_h^{UP*}(v) = \begin{cases} v & \text{if:} \quad d_{h+l} < v \leq v^{UP/H|S} \\ V_h[\frac{\partial DTC}{\partial V_h} = 0] & \text{if:} \quad v > v^{UP/H|S} \end{cases} \tag{24}$$

4.1.1. Defining the capacity allocation ranges

Summarising the results of Case 1 and 2, the profit maximising spatial allocation is given by the following section-wise defined function:

$$V_h^{UP*}(v) = \begin{cases} v & \text{if:} \quad v \leq v^{UP/H|S} \\ V_h[\frac{\partial DTC}{\partial V_h} = 0] & \text{if:} \quad v > v^{UP/H|S} \end{cases} \tag{25}$$

For VRE penetrations below $v \leq v^{UP/H|S}$ capacity is allocated only to the high-availability node. I denote this range as *high-availability deployment range*. For higher VRE penetration levels ($v > v^{UP/H|S}$), producers split the capacity among the two nodes. This range I denote as *split capacity deployment range*.

4.1.2. Inefficiencies resulting from UP

Allocation is efficient when the highest usable supply possible for a given VRE penetration is achieved. Such a usable supply is achieved under nodal pricing, which I denote with $US^{NP}(v)$. For some VRE penetration levels (v) the allocation under uniform pricing differs from the efficient allocation, resulting in a lower usable supply (denoted with US^{UP}). This can be explained as follows: As $t < d_i \forall i$ by assumption (see Chapter 2) the actual curtailment at node h exceeds the commercial curtailment. Hence, there is a lower incentive for producers to allocate capacity to node l under uniform pricing compared to nodal pricing. As

a result, producers allocate capacity to node h for higher VRE penetration levels under uniform pricing compared to nodal pricing (i.e., $v^{UP/H|S} > v^{H|L}$).

When VRE penetration is sufficiently low (i.e., $v \leq v^{H|L}$) capacity is allocated to node h under uniform and nodal pricing, such that the usable supply is identical under both regimes and inefficiencies are absent. For $v > v^{H|L}$ inefficiencies occur. The resulting welfare loss is given by the reduction in usable supply compared to the optimum times the marginal costs for conventional technology:

$$\text{Welfare Loss}(v) = \big(US^{NP}(v) - US^{UP}(v)\big)c \tag{26}$$

As the global VRE share is given by dividing the usable supply with the global demand, the following relationship between the welfare loss and the reduction in the global VRE share exists:

$$\text{Reduction in global VRE share}(v) = \frac{\text{Welfare Loss}(i)}{d_{h+l} \cdot c} \tag{27}$$

Welfare loss increase with increasing v as long as producers solely allocate capacity to node h, i.e. for $v^{H|L} < v \leq v^{UP/H|S}$.

When capacity is split among the two nodes (i.e., *split capacity deployment range* which is valid for $v > v^{UP/H|S}$), welfare losses are partly mitigated. This is because capacity allocated to node l is not curtailed, such that the average marginal usable supply of both nodes exceeds the marginal usable supply under nodal pricing.

End of Explanation.

Figure 8 demonstrates the insights from Finding UP 1 numerically.[18] The parameters are identical to Figure 2. By setting $c = \frac{1}{d_{h+l}}$, the welfare loss coincides with the reduction in the global VRE share.

The upper diagram shows that capacity is allocated solely to the high-availability node when $v < 5.1 d_{h+l}$. Welfare losses arise for $v > v^{H|L}$, where $v^{H|L}$ defines the value separating the *high-* and *low-availability deployment range* under nodal pricing. For $v > v^{H|L}$ the marginal usable supply of node h subceeds the one of node l, such that welfare would be increased when some VRE would be shifted to node l. The welfare losses grow with increasing VRE penetration. At $v = 5.1 d_{h+l}$, welfare losses reach their maximum. Due to the inefficient allocation, less than 55% of demand can be served with VRE, compared to 75% under an

[18]The optimisation problem solved numerically to generate this and the remaining figures in this chapter resembles the optimisation problem described in Chapter 2 and solved in this chapter. Differences in the formulation arising from using a numerical instead of an analytical approach are described in Appendix D.

optimal allocation. Hence, conventional power needs to serve an additional 20% of demand, inducing costs of $0.2d_{h+l}c = 0.2$. This is the case even though the potential supply of VRE is 20% higher under uniform pricing than under nodal pricing. These numbers imply 65% of VRE is curtailed on average and 95% of marginal supply is curtailed.

When $v > 5.1d_{h+l}$ capacity is split among the nodes h and l in a roughly 70/30 ratio. As no supply is curtailed at node l, welfare losses compared to the social optimum slightly decline.

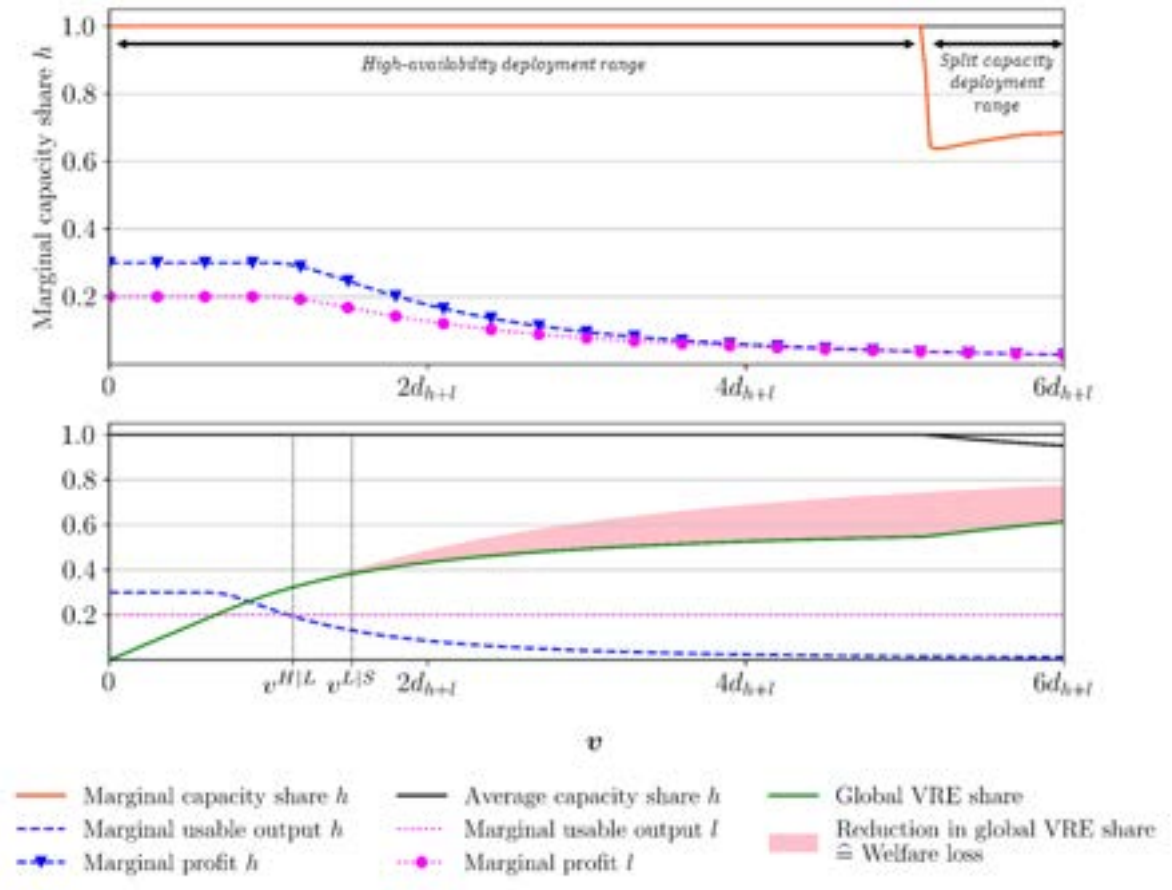

$v^{H|L}$ and $v^{L|S}$ mark the cut-off points between respective ranges arising under nodal pricing.

Figure 8: Spatial allocation, marginal usable and saleable supply, VRE shares and welfare losses at different VRE penetration levels under uniform pricing.

4.2. Effects of changes in the transmission capacity and demand distribution

In this subchapter, I derive the effect of changes in the transmission capacity t and the demand distribution on the capacity allocation and welfare. Based on the analysis, I conclude:

Finding UP 2. *Under uniform pricing, the transmission capacity and the demand distribution do not*

affect the capacity allocation. With increasing t, welfare losses decrease. Allocation is efficient when $t > d_i$. Distributing demand more according to potential supply also reduces welfare losses.

Explanation. The transmission capacity and the demand distribution do not affect the capacity allocation. This is because curtailment arising from network restrictions is ignored under uniform pricing.

As curtailment arising from network restrictions affect the socially optimum capacity allocation, the transmission capacity and the demand distribution affect the efficiency. The deployment under uniform pricing coincides with the one under nodal pricing, when transmission capacity allows to serve the demand at node l, even when capacity is allocated solely at node h, i.e., $t > d_i$. Hence, welfare losses are absent when $t \geq d_i$. For such level of t the commercial curtailment ($\overline{K^c}$) and the physical curtailment (K) coincide. With decreasing t, welfare losses increase. This is because with decreasing t, it is optimal to allocate more capacity to node l to reduce curtailment.

Distributing nodal demand more according to potential supply reduces the need for transmission. Hence, distributing demand more according to potential supply also reduces the level of curtailment arising from network restrictions and welfare losses.

End of Explanation.

Figure 9 displays the effect of changes in the transmission capacity and the demand distribution.[19]

Independent of the transmission capacity and the demand distribution, capacity is allocated to node h until $v = 5.1 d_{h+l}$. For the same VRE penetration level, welfare losses are highest. The welfare loss decreases with increasing t. For low transmission capacity, i.e., $t = \frac{1}{4} d_{h+l}$, welfare losses equivalent to the variable costs, when serving 20% of global demand with conventional power, occur. The welfare loss is more than halved when transmission capacity is tripped, and welfare losses disappear for $t > d_i$. Furthermore, the higher t, the later welfare losses emerge.

[19]The parameters in Figure 9a are identical to Figure 3, while the parameters in Figure 9b are identical to Figure 4. By setting $c = \frac{1}{d_{h+l}}$, the welfare loss coincides with the reduction in VRE share.

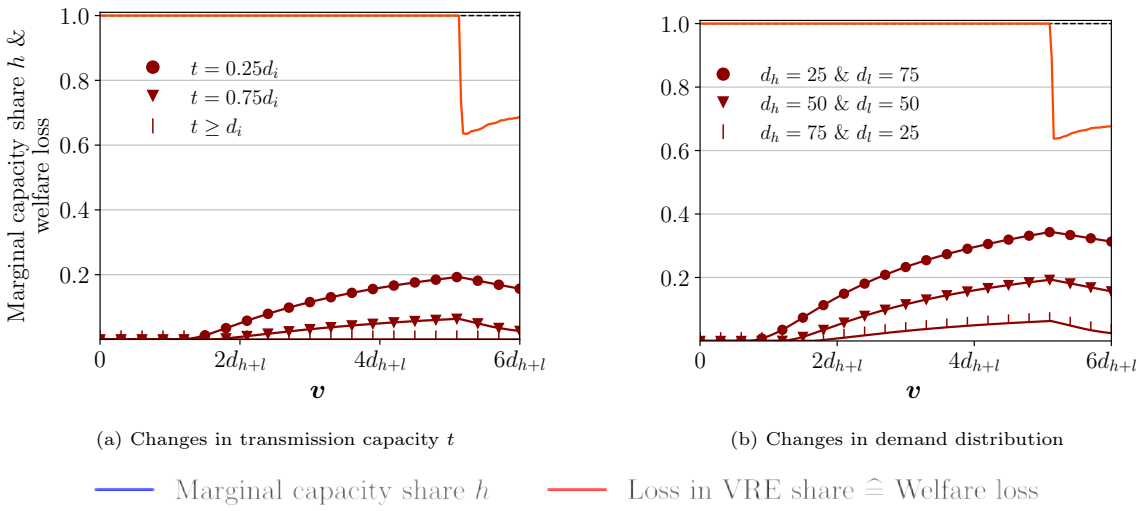

(a) Changes in transmission capacity t

(b) Changes in demand distribution

Figure 9: Effects of changes in the transmission capacity and demand distribution on the spatial allocation ranges and welfare losses under uniform pricing.

With demand increasingly located at node h, the welfare losses decreases. When 75% of demand is located at node h, welfare losses are only one-fifth compared to the case when 75% of demand is located at node l.

4.3. Effect of changes in the availability profiles

In this chapter, I derive the effects arising from different features of the availability profiles on the ranges of the capacity allocation under uniform pricing. To do so, I analyse the effects of changes in the correlation among nodal availability profiles and changes in the average and the variance of nodal availability profiles. Based on the analysis, I conclude:

Finding UP 3. *Under uniform pricing, the availability profiles affect the spatial allocation. The effect on the high-availability deployment range and the split capacity deployment range is identical to the case of nodal pricing and $t \geq d_i$. For $t < d_i$, the effect on the spatial allocation are stronger under uniform pricing. Changes in the availability profiles, which incentivise capacity to be allocated more according to demand, reduce welfare losses.*

Explanation. The availability profiles affect the spatial allocation because the global supply is affected. The effect on the spatial allocation of VRE is stronger than under nodal pricing if transmission capacity is binding. This is because, under nodal pricing the effects on the capacity allocation arising from availability profiles are mitigated by curtailment arising from limited transmission capacity. The higher t, the lower the mitigation

and the higher the impact of availability profiles. For $t \geq d_i$, the availability profiles affect the allocation in the same way under uniform and nodal pricing.

Changes in the availability profiles also affect the level of inefficiency. If changes in the availability profiles incentivise a capacity allocation which induces potential supply to be allocated more according to demand, welfare losses are reduced. This is because, with the increasing alignment of potential nodal supply and nodal demand, less potential supply needs to be transmitted, and less supply is curtailed due to limited transmission capacity. Thereby the redispatch-level of conventional power plants decreases, reducing costs and increasing welfare and the global VRE share. Depending on the demand distribution, the availability profiles, which minimise the welfare loss differ.

End of Explanation.

4.3.1. Correlation

When availabilities are perfectly correlated, producers allocate capacity solely to the high-availability node. The lower the correlation, the more often the availability at node l exceeds the availability at node h. Producers exploit these differences in the availability profile by allocating some capacity to node l. Hence, with decreasing correlation, producers allocate more capacity to node l. The effect on welfare depends on the demand distribution. When demand $d_l \geq d_h$, decreasing the correlation decreases the need for transmission and curtailment arising from limited transmission capacity. Hence, low $\rho_{h,l}$ lead to low welfare losses compared to the social optimum. However, when demand is located mainly at node h, the need for transmission is lowest, and resulting curtailment is lowest when the correlation is high. Hence, high $\rho_{h,l}$ lead to low welfare losses compared to the social optimum.

Figure 10 illustrates these results.[20] Capacity is solely allocated to node h for all levels of analysed VRE penetration when availability profiles are perfectly correlated. In contrast, when availability profiles are uncorrelated, 38% to 100% of marginal VRE capacity is allocated to node l for $v > 2.5d_{h,l}$. Which level of correlation yields the lowest welfare loss depends on the demand distribution. When demand is equally distributed, welfare losses are lowest when availability profiles are uncorrelated. In contrast, when 95% of demand is concentrated at node h, welfare loss remains absent in the analysed VRE penetration domain when the correlation is perfect.

[20]The average and the variance of the availability profiles are identical to Figure 8. To better identify the effect on welfare losses, $t = 5$ is assumed. By setting $c = \frac{1}{d_{h+l}}$, the welfare loss coincides with the reduction in the VRE share.

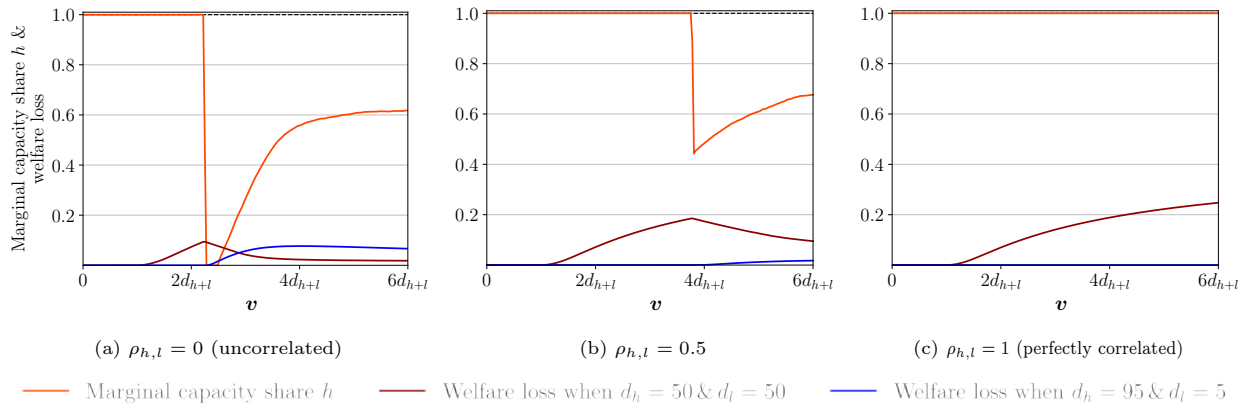

Figure 10: Effect of the correlation among availability profiles on the spatial allocation ranges and welfare losses under uniform pricing.

4.3.2. Average

Under uniform pricing, a higher average nodal availability incentivises producers to allocate more VRE capacity to the respective node. This is because producers only consider the increase in the potential nodal supply. The increasing curtailment arising from limited transmission capacity are ignored. As $\mu_h > \mu_l$, producers allocate more capacity to node h. With an increasing difference in availabilities the share of capacity allocated to node h increases.

Hence, when demand $d_l \geq d_h$, decreasing the differences in availability decreases the need for transmission and hence decreases the welfare loss. However, when demand is concentrated at node h, the need for transmission and the resulting welfare losses from curtailment is lowest when differences in availability are substantial.

Figure 11 illustrates these results.[21] Capacity is solely allocated to node h for all levels of analysed VRE penetration when the average availability at node h is 2.3 times as high than at node l (i.e., $\mu_h = 0.35$ and $\mu_l = 0.15$). In contrast, 40-100% of marginal VRE capacity is allocated to node l for $v > 1.9d_{h,l}$, when the average availability at node h is only 17% higher than at node l (i.e., $\mu_h = 0.27$ and $\mu_l = 0.23$).

Which nodal average availabilities yield the lowest welfare loss depends on the demand distribution. When demand is equally distributed, welfare losses are lowest when average availabilities barely differ. In contrast, when 95% of demand is concentrated at node h, welfare losses remain absent in the analysed VRE penetration domain when availabilities are 2.3 times higher at node h than at node l.

[21]The variance of the availability profiles varies between X and Y, which is very close to the variance assumed in Figure 10. To better identify the effect on welfare losses, a low transmission capacity of $t = \frac{d_{h+l}}{10}$ and a moderate correlation of $\rho_{h,l} = 0.4$ is assumed. By setting $c = \frac{1}{d_{h+l}}$, the welfare loss coincides with the reduction in VRE share.

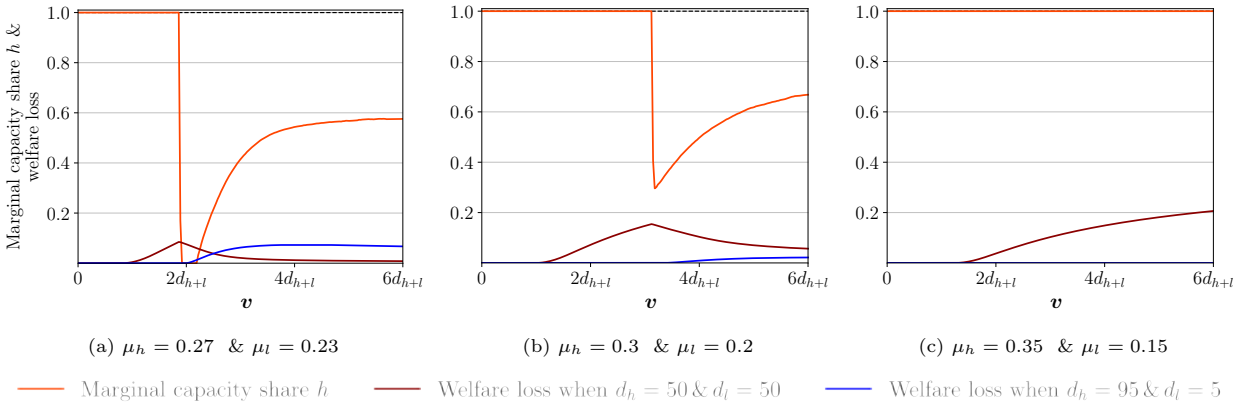

Figure 11: Effect of the average availability on the spatial allocation ranges and welfare losses under uniform pricing.

4.3.3. Variance

Under uniform pricing, a higher nodal variance incentivises producers to allocate less VRE capacity to the respective node. This is because, with increasing nodal variance, the potential nodal supply exceeds the global demand is higher share of periods. In such periods, prices are zero, and some potential supply cannot be sold. To reduce the share of such situations, producers allocate less VRE to the node with increased variance.

Hence, when demand $d_l \geq d_h$, increasing the variance at node h or decreasing the variance at node l decreases the need for transmission and curtailment arising from limited transmission capacity. Such changes in the variance also decrease the welfare loss compared to the social optimum. When demand is concentrated at node h, the need for transmission and the resulting welfare losses from curtailment is lowest when the variance at node h is low compared to the variance at node l.

These results are illustrated in Figure 11.[22] Capacity is solely allocated to node h for all levels of analysed VRE penetration when availability profiles at both nodes share the same variance (i.e., $\sigma_h = \sigma_l = 0.2$). In contrast, 65-100% of marginal VRE capacity is allocated to node l for $v > 3d_{h,l}$, when the variance at node h is 50% higher than at node l (i.e., $\sigma_h = 0.24$ and $\sigma_l = 0.16$).

Which nodal variances yield the lowest welfare loss depends on the demand distribution. When demand is equally distributed, welfare losses are lowest when the variance is 50% higher at node h. In contrast, when 95% of demand is concentrated at node h, welfare losses remain absent in the analysed VRE penetration domain when the variance is identical at both nodes.

[22]The assumed average in the availability profiles is identical to Figure 7, and the assumed transmission capacity, correlation, as well as variable costs of the conventional technology, are identical to Figure 11.

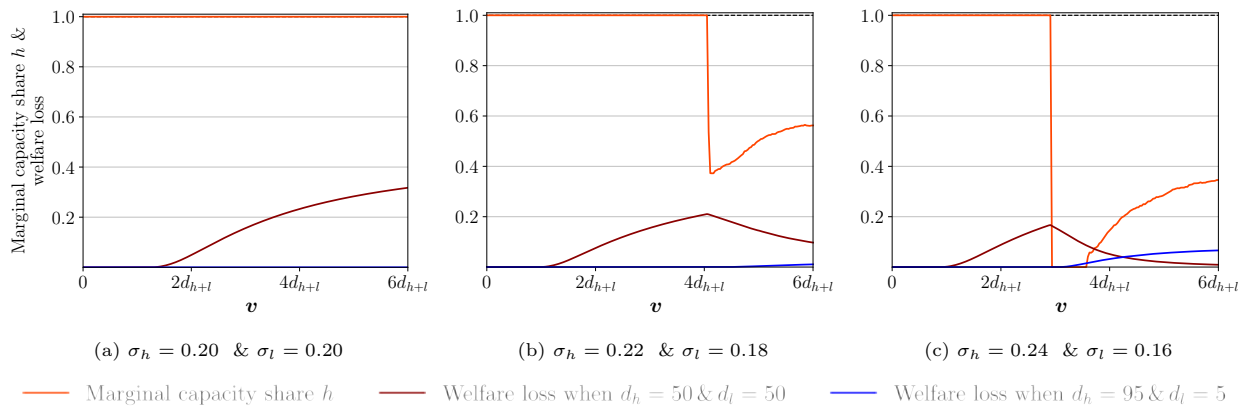

Figure 12: Effect of the average availability on the spatial allocation ranges and welfare losses under uniform pricing.

5. Discussion

This paper shows that optimal VRE allocation can be grouped into three ranges. At low levels of VRE penetration, capacity should be allocated to the node with higher average availability (i.e. *high-availability deployment*). When curtailment fully removes the advantage in usable supply of the high-availability node, marginal capacity should be allocated to the node with lower availability (i.e., *low-availability deployment range*). When curtailment is present at both nodes, marginal capacity should be split (i.e., *split capacity deployment range*). Policymakers designing instruments to expand the VRE capacity should consider the range they are in. Countries starting to deploy in VRE should incentivise the placement of initial capacities in regions with high availability. Countries that already have significant VRE capacity in regions with a high average availability may be better off when incentivising (some) investment in regions with lower availability.

The width of the *high* and the *low-availability deployment range*, as well as the nodal capacities shares in the *split capacity deployment range*, are found to depend on the transmission capacity, the demand distribution, and the availability profiles. These characteristics vary among countries. In the UK, compared to Germany, the average wind availability is higher, the regional difference is lower, and the correlation among the availability profiles is lower (Staffell and Pfenninger, 2016; Sinden, 2007). As a result, the *high* and *low-availability deployment range* are narrower in the UK than in Germany due to lower differences in availability and higher average availabilities when assuming similar transmission capacity and demand distribution.

Under uniform pricing, the dominant market design, producers are found to allocate capacity to the high-availability node for higher VRE penetration levels than socially optimal. This is because curtailment arising from limited transmission capacity, which would encourage producers to allocate capacity more

according to demand, is ignored. Welfare losses occur when curtailment from limited transmission capacity fully diminish the advantage in usable supply of the high-availability node. The welfare losses increase until differences in availability profiles incentivise allocating some capacity to the low-availability node.

Hence, countries with uniform pricing that start to deploy VRE or feature low VRE shares do not have to implement additional measures to improve the spatial allocation. In line with the findings of this paper, in Japan, VRE only serves 6% of demand, and support schemes do not differentiate spatially (IEA, 2022a). Countries with uniform pricing, which already deploy substantial VRE capacity, such as Germany, should consider measures encouraging producers to invest in areas with lower availabilities.

The welfare losses under uniform pricing decreases in the level of transmission capacity and increases in the need for transmission. The latter is found to be influenced by the demand distribution and the availability profiles. Welfare losses are, for instance, small when transmission capacity is high compared to nodal demand or demand is allocated mainly to the high-availability node. In contrast, welfare losses are found to be high when transmission capacity is low, demand is concentrated in the low-availability node and availability profiles incentive an allocation to the high-availability node (e.g., high difference in nodal availabilities). Such circumstances are, for example, present in Germany. This is in line with the finding from ACER (2022), who show that splitting Germany into two market zones would yield larger welfare increases than splitting market zones in other EU countries.[23] Hence, policymakers should take into account the given transmission capacities, the demand distribution, and regional availability profiles when considering to split their market zone or to implement spatially differentiated VRE subsidies.

The findings of my analysis confirm and extent the findings of the papers presented in Chapter 1. The results of Kies et al. (2016) suggest that with an increasing VRE penetration, it is optimal to increasingly allocate capacity to regions with a low average availability. My findings extend the result by showing that the optimal spatial allocation of VRE can be grouped into three ranges.

Pechan (2017) finds that under nodal pricing, producers increasingly concentrate capacity at high-availability nodes when the correlation increases and when the variance in high-availability nodes is low. This is in line with my analysis. My research adds the finding that the effect of correlation becomes more relevant with increasing transmission capacity.

In the case of uniform pricing, Pechan (2017) does finds no effect of correlation and variance on the allocation under uniform pricing. This is because she only analyses a case with a moderate VRE share. I can

[23]Splitting a country into two market zones allows prices to differ when transmission capacities between the new market zones are congested. Such a market design is an intermediate design of uniform pricing and nodal pricing.

show that the capacity allocation is affected once the VRE penetration reaches a certain threshold.

In line with my analysis, a welfare loss arises in Schmidt and Zinke (2020) due to an inefficient allocation of VRE. The identified welfare loss of 1.5% seems low compared to numerical results in my analysis. This is because, in my analysis, a case with similar correlation, similar demand distribution and similar VRE penetration leads to a welfare loss of roughly 15%. [24] The difference in welfare loss mainly arises due to the following two aspects: First, Schmidt and Zinke (2020) only assess the allocation of wind onshore capacities added in the years 2020 to 2030. These capacities produce less than 20% of the VRE supply. The remaining 80% come from onshore wind built before the year 2020, offshore wind and solar power. These capacities are distributed identically under uniform and nodal pricing in their analysis. Second, Schmidt and Zinke (2020) consider regional VRE potentials, which limit the capacity allocation to regions with a high average availability. This limitation increases the capacity allocation to nodes with lower average availability under uniform pricing compared to my analysis. Hence, if the authors would ignore limited potentials and allocate all VRE capacities, welfare losses would likely be substantially higher.

The model's simplicity allows to fundamentally understand the effect of crucial system topology parameters on the spatial allocation of VRE, and the inefficiencies arising under uniform pricing. Despite the model's simplicity, I consider main elements which influence the spatial allocation. While the rationales I identify should remain, additional effects may occur when considering a more realistic setting. In the following paragraphs I discuss central simplifications and potential impacts.

I model the spatial allocation decision as a one-shot game in which producers can observe a fixed system topology. Based on this topology, producers allocate capacity between the two nodes. In reality, the parameters of the system topology, such as VRE penetration, transmission capacity and demand distribution, change continuously over time in a dynamic process. If only the VRE capacity increases continuously over time, the three ranges identified can be translated into three phases. Namely, initial VRE capacity is allocated at the high-availability node, then capacity is allocated at the low-availability node, and when a high VRE penetration level is reached, capacity is split between the two nodes. In the more likely case of multiple parameters evolving over time, the optimal spatial allocation becomes much more complex. A still simple example could be a continuous increase in VRE capacity and a discrete transmission capacity at one point in time. In such a case, generators allocating VRE capacity need to consider the proportion of the lifetime of the plant before and after the increase in transmission capacity. A possible outcome could be that in a period

[24] In Figure 10b the case with a 25% demand allocation to high-availability node and a VRE penetration of $2d_{h+l}$ roughly depicts the setting in Schmidt and Zinke (2020).

with moderate VRE penetration, which is well before the transmission capacity increase, it is optimal to allocate a high proportion of capacity to the low-availability node. As the date of the transmission capacity increase approaches, it would be optimal to increasingly allocate VRE capacity to the high-availability node. In reality, therefore, the three ranges identified are unlikely to translate into three phases of capacity expansion. Nevertheless, the results improve the general understanding of the impact of changes in the system topology on the spatial allocation of VRE.

Second, to ensure an analytical solution and to gain a profound theoretical understanding I do not analyse the effect of storage and demand flexibility in the model. However, storage and demand flexibility represents important elements of the system topology and influence the spatial allocation of VRE. This is because storage and demand flexibility provide means to better align VRE supply with demand, by shifting the time of supply provision or shifting the time of demand. The IEA (2022b) assumes storage and demand flexibility to provide a quarter of the required flexibility each in the year 2050 in the Announced Policy Scenario. In my model, storage operators would maximise profits by injecting during periods of high VRE supply (i.e., VRE technology sets the price) and withdrawing during periods of low VRE supply (i.e., conventional technology sets the price). Similarly, operators of demand flexibility would maximise profits form flexibility when shifting demand from periods with high VRE supply to periods with low VRE supply. This implies, with increasing storage and demand flexibility the sum of supply from VRE and storage minus flexible demand becomes less volatile. This is similar to a decrease in the variance of the availability profile. An increase in flexible capacity should therefore have similar effects like a decrease in the variance, which I analyse in Chapter 3 and 4. Czock et al. (2022), who analyse the optimal storage allocation find storage to be predominantly built at transmission bottlenecks, such that curtailment before bottlenecks decreases. This corresponds to building storage capacity mainly at the high-availability node in my model. Considering such a spatial allocation of storage would increase in the VRE capacity at the high-availability node for most VRE penetration levels compared to my analysis.

Furthermore, I only consider a two-node network. Considering a complex network with multiple nodes yield supply to be transported via multiple nodes. These nodes' remaining available transmission capacity is reduced in such a case. Hence, in case of multiple nodes, not only does the transmission capacity of the producing or importing node affect the spatial allocation of VRE, but also the transmission capacity of all nodes in between.

Furthermore, the analysis only considers one VRE technology and one conventional technology. In most countries, at least two VRE technologies, namely wind and solar, are employed. The coexistence of the VRE

technologies likely induces additional interaction effects. For instance, when demand is regionally equally distributed, solar conditions are similar across a country, and wind capacities are located mostly in the north, it would be optimal to allocate more solar capacity to the south than to the north. In contrast, it would be optimal to allocate solar capacity would be predominantly to the north, when most wind capacities are located in the south. Thereby the effects also depend on the penetration level of each VRE technology and the correlation of availabilities among the different VRE technologies. Similar dependencies likely arise from multiple conventional technologies with differing variable costs.

Another simplification is the assumption of constant and inelastic demand. In reality, demand is neither constant nor inelastic. Instead, demand is fluctuating and slightly positively correlated with VRE availability. This is because demand tends to be higher during the day than at night, which is also the case for solar availability. Demand also tends to be higher in winter than in summer, which is also the case for wind availability. Furthermore, household and industrial electricity demand features some level of price elasticity (Cialani and Mortazavi, 2018). Taking such demand characteristics into account is likely to affect the results under nodal pricing in the following way: The *high-availability deployment range* is likely to be valid also for higher VRE penetration levels. First, because curtailment at node h would be lower due to the positive correlation between demand and VRE availabilities. And second, because the remaining curtailment would be partly offset by an increase in elastic demand due to the lower average price level at node h. The *low-availability deployment range* is likely to be narrowed. This is because the range cut-off point is reached when curtailment occurs at node l, and with non-constant demand, low demand may coincide with high VRE availabilities, triggering curtailment. Under *split capacity deployment range*, the share of capacity allocated to the high-availability node is likely to increase if elastic demand is considered. This is because average prices at node h are on average lower than at node l, so the share of demand at node h increases. The increase in demand translates into an increase in electricity prices at node h, which then increases the willingness of investors to allocate capacity to node h.

Considering demand elasticity would also yield in demand being lower under uniform compared to nodal pricing for higher VRE penetration levels. This is because consumers on average bear higher electricity prices under uniform pricing due to the less efficient spatial allocation of VRE and the assumption that the costs for redispatch are borne by the electricity consumers. In addition, due to the lack of a regional price signal under uniform pricing, the regional distribution of demand would be less consistent with the VRE production compared to the case under nodal pricing.

While the two most common market designs are uniform and nodal pricing, the exact regulation usually

differs from the two cases I analyse. A prominent example is the compensation of VRE capacity in case of redispatch under uniform pricing. I assume, like Schmidt and Zinke (2020) and Pechan (2017), curtailed producers of VRE are compensated with the market price. In some countries, like Spain, the compensation of VRE capacity in case of redispatch is below market prices, such that producers consider the curtailment, when deciding on the spatial allocation (Bird et al., 2016). The lower the compensation, the closer the capacity allocation to the one arising under nodal pricing. However, studies that analyse the effects of reduced compensations on spatial allocation are lacking. Such studies would get increasingly relevant as countries, such as the UK, consider reducing their compensations (Cholteeva, 2020).

6. Conclusion

To date, there is a lack of theoretical literature that provides a comprehensive understanding of the implications of VRE allocation. This paper contributes to this research gap by developing a theoretical model that depicts the spatial allocation of VRE in a two-node network. Using the model, I analyse under which conditions it is welfare enhancing to allocate some VRE capacity to locations with unfavourable potential supply. Furthermore, I assess how the spatial allocation under uniform pricing differs from the optimum and derive the resulting welfare effects.

From a theoretical perspective, my contribution is threefold: First, I show analytically that the optimal spatial allocation can be grouped into three spatial allocation ranges. Second, I show how the width of each range and the allocation when capacity is split is determined by the different parameters of the system topology. And third, I identify the allocation under uniform pricing and the resulting welfare loss, and show how the welfare loss is affected by the different parameters of the system topology. In addition, my study can assist policymakers when designing policies that affect the spatial allocation, or investors trying to identify the profit-maximising allocation of VRE investments.

I develop a stylised model which provides a fundamental understanding of the dynamics and interactions in the allocation of VRE. However, additional effects are likely to occur when considering a setting with a realistic network, multiple VRE and conventional technologies, as well as storage and demand elasticity. The same holds true when considering endogenous investments not only in VRE but also in additional technologies, such as transmission capacity. Taking into account real-world constraints, such as limited regional VRE potentials, is likely to reduce the inefficiencies observed under uniform pricing.

Further research could extend the model to include additional technologies. For example, investigating a second VRE technology would allow understanding the interdependencies of expanding wind and solar capacity

at the same time. The inclusion of elastic demand and storage would allow the analysis of how flexibility affects the spatial distribution of VRE. It could also identify combinations of VRE and storage capacity sufficient to meet all demand with VRE. The implementation of endogenous investments in transmission capacity would make it possible to identify the effects of such investments on the spatial allocation of VRE. This would provide insights into the trade-off between a network-friendly allocation of VRE and the expansion of transmission capacity. Finally, the implementation of a more realistic network would allow to study the impact of curtailment occurring at nodes between production and consumption nodes on the spatial allocation.

Acknowledgements

The author would like to thank Christian Tode and Marc Oliver Bettzüge for their thoughtful and constructive comments and discussions on this work. Additionally, I would like to thank Berit Czock and Felix Schäfer for their helpful comments. The paper also benefited from discussions at the 29$^{\text{th}}$ YEEES Seminar 2022 in Ghent. The author conducted this work in the Hans-Ertel-Centre for Weather Research framework, funded by the German Federal Ministry for Digital and Transport (grant number BMVI/DWD 4818DWDP5A). The content of this paper reflects the opinions of its author only and not those of EWI.

Appendix A. Properties of curtailment due to limited transmission capacity

Curtailment (K) can arise due to limited transmission capacity (K_i^t) and due to global potential supply exceeding global demand excluding the curtailment due to limited transmission capacity (K^d). In this section the properties of curtailment due to limited transmission capacity (K_i^t) are assessed.

Appendix A.1. Functional form of curtailment

Curtailment from limited transmission capacity (K_i^t) arises when for at least one period r the potential supply exceeds the nodal demand plus transmission capacity (i.e., $V_i \cdot avail_{i,r} > d_i + t$). Otherwise, there is no curtailment arising from limited transmission capacity. As the beta distribution describes the deterministic distribution of the availabilities, K_i^t can be expressed as follows:

$$K_i^t = \int_0^1 \max\left\{0, \underbrace{(x - \frac{(d_i + t)}{V_i})V_i}_{\text{level of curtailment}} \cdot \underbrace{\frac{1}{B(\alpha_i, \beta_i)} x^{\alpha_i - 1}(1-x)^{\beta_i - 1}}_{\text{availability density}}\right\} dx \tag{A.1}$$

For all $x < \frac{d_i+t}{V_i}$ the second element of the $max\{\}$ function is negative, such that the $max\{\}$ function returns 0. Hence, the curtailment from limited transmission capacity can be rewritten as follows:

$$K_i^t = \begin{cases} 0 & \text{if } V_i \leq d_i + t \\ \int_{\frac{d_i+t}{V_i}}^{1} (x - \frac{(d_i+t)}{V_i}) V_i \frac{1}{B(\alpha_i,\beta_i)} x^{\alpha_i - 1}(1-x)^{\beta_i - 1} dx & \text{if } V_i > d_i + t \end{cases} \tag{A.2}$$

Appendix A.2. Marginal curtailment given all capacity is allocated to node h

In this section I derive the marginal curtailment at node h when marginally increasing the VRE penetration v given that all capacity is allocated to node h (i.e., $K_h^t\big|_{V_h=v}$). To do so I substitute V_h with v in a first step:

$$K_h^t\Big|_{V_h=v} = \begin{cases} 0 & \text{if } v \leq d_h + t \\ \int_{\frac{d_h+t}{v}}^{1} (x - \frac{(d_h+t)}{v}) v \frac{1}{B(\alpha_h,\beta_h)} x^{\alpha_h - 1}(1-x)^{\beta_h - 1} dx & \text{if } v > d_h + t \end{cases} \tag{A.3}$$

In a second step I derive $\frac{\partial K_h^t}{\partial v}\big|_{V_h=v}$: For $v \leq d_h + t$ the derivative of $\frac{\partial K_h^t}{\partial v}\big|_{V_h=v}$ is zero.

To calculate the derivative of $\frac{\partial K_h^t}{\partial v}\big|_{V_h=v}$ for $v > d_h + t$ I first rewrite K_h^t, such that the finite integral is solved:

$$K_h^t\Big|_{V_h=v} = \frac{\alpha_h}{\alpha_h+\beta_h} v + \frac{(d_h+t) B_{\frac{d_h+t}{v}}(\alpha_h,\beta_h) - v B_{\frac{d_h+t}{v}}(1+\alpha_h,\beta_h)}{B(\alpha_h,\beta_h)} - (d_h+t) \tag{A.4}$$

This expression is then used to calculate the derivative of $\frac{\partial K_h^t}{\partial v}\big|_{V_h=v}$ for $v > d_h + t$:

$$\frac{\partial K_h^t}{\partial v} = \frac{\alpha_h}{\alpha_h+\beta_h} - \frac{B_{\frac{d_h+t}{v}}(1+\alpha_h,\beta_h)}{B(\alpha_h,\beta_h)} \tag{A.5}$$

Combining the results for the two sections, $\frac{\partial K_h^t}{\partial v}\big|_{V_h=v}$ can be expressed by:

$$\frac{\partial K_h^t}{\partial v}\Big|_{V_h=v} = \begin{cases} 0 & \text{for: } v \leq d_h + t \\ \frac{\alpha_h}{\alpha_h+\beta_h} - \frac{B_{\frac{d_h+t}{v}}(1+\alpha_h,\beta_h)}{B(\alpha_h,\beta_h)} & \text{for: } v > d_h + t \end{cases} \tag{A.6}$$

For $v > d_h + t$ and valid parameter values (i.e., $\alpha_h, \beta_h, d_h + t > 0$) the marginal curtailment $\frac{\partial K_h^t}{\partial v}\Big|_{V_h=v}$ is strictly positive. This is because $\frac{\alpha_h}{\alpha_h+\beta_h} > \frac{B_{\frac{d_h+t}{v}}(1+\alpha_h,\beta_h)}{B(\alpha_h,\beta_h)}$ for the valid parameter values. Further, the marginal curtailment ($\frac{\partial K_h^t}{\partial v}\Big|_{V_h=v}$) strictly increases in v. This is because $B_{\frac{d_h+t}{v}}(1+\alpha_h,\beta_h)$ strictly decreases in the VRE penetration (v) for valid parameter configurations, while all other elements of Equation A.6 are

independent of v.

Appendix A.3. Effect of various parameters on marginal curtailment

In this section I access the effect of the transmission capacity (t), the demand distribution (d_h), and the average availability on marginal curtailment evaluated at $V_h = v$. To do so I take the derivative of $\frac{\partial K_h^t}{\partial v}\big|_{V_h=v}$ with respect to respective parameter.

Appendix A.3.1. Effect of transmission capacity

The derivative of $\frac{\partial K_h^t}{\partial v}\big|_{V_h=v}$ with respect to the transmission capacity (t) is given by:

$$\frac{\partial^2 K_h^t}{\partial v\,\partial t}\bigg|_{V_h=v} = \begin{cases} 0 & \text{for: } v \leq d_h + t \\ -\dfrac{(\frac{d_h+t}{v})^{\alpha_h}(1-\frac{d_h+t}{v})^{-1+\beta_h}}{vB(\alpha_h,\beta_h)} & \text{for: } v > d_h + t \end{cases} \tag{A.7}$$

For $v > d_h + t$ and valid parameter values (i.e., $\alpha_h, \beta_h, d_h + t > 0$) the term $\frac{\partial^2 K_h^t}{\partial v\,\partial t}\Big|_{V_h=v}$ is strictly negative. This implies that marginal curtailment when marginally increasing v evaluated at $V_h = v$ increases at a lower rate with increasing t.

Appendix A.3.2. Effect of demand distribution

The global demand d_{h+l} is split into the nodal demands d_h and d_l. However, only d_h affects the marginal curtailment evaluated at $V_h = v$ (see Equation A.6).

Hence, I analyse how increasing d_h affects the marginal curtailment by taking the derivative of $\frac{\partial K_h^t}{\partial v}\big|_{V_h=v}$ with respect to the demand at node h:

$$\frac{\partial^2 K_h^t}{\partial v\,\partial d_h}\bigg|_{V_h=v} = \begin{cases} 0 & \text{for: } v \leq d_h + t \\ -\dfrac{(\frac{d_h+t}{v})^{\alpha_h}(1-\frac{d_h+t}{v})^{-1+\beta_h}}{vB(\alpha_h,\beta_h)} & \text{for: } v > d_h + t \end{cases} \tag{A.8}$$

For $v > d_h + t$ and valid parameter values (i.e., $\alpha_h, \beta_h, d_h + t > 0$) the term $\frac{\partial^2 K_h^t}{\partial v\,\partial d_h}\Big|_{V_h=v}$ is strictly negative. This implies that marginal curtailment when marginally increasing v evaluated at $V_h = v$ increases at a lower rate with increasing d_h.

Appendix A.3.3. Effect of average availability

The availability is described by the parameters α_h and β_h. As stated in Chapter 2, increasing α_h primarily increases the average availability, while the variance remains rather constant. To assess the effect of changes

in the average availability, I analyse the effects arising from changes in α_h. However, only α_h affects the marginal curtailment evaluated at $V_h = v$ (see Equation A.6).

Hence, I analyse how increasing α_h affects the marginal curtailment by taking the derivative of $\frac{\partial K_h^t}{\partial v}\big|_{V_h=v}$ with respect to α_h:

$$\frac{\partial^2 K_h^t}{\partial v \partial \alpha_h}\bigg|_{V_h=v} = \begin{cases} 0 & \text{for: } v \leq d_h + t \\ \frac{\beta_h}{(\alpha_h+\beta_h)^2} & \\ \quad - \frac{B_{\frac{d_h+t}{v}}(\alpha_h+1,\beta_h)\left(\log\left(\frac{d_h+t}{v}\right)+\psi^{(0)}(\alpha_h+\beta_h)-\psi^{(0)}(\alpha_h)\right)}{B(\alpha_h,\beta_h)} & \text{for: } v > d_h + t \\ \quad + \frac{\left(\frac{d+t}{v}\right)^{\alpha_h} {}_3F_2\left(\alpha_h+1,\alpha_h+1,1-\beta_h;\alpha_h+2,\alpha_h+2;\frac{d+t}{v}\right)}{\frac{v(1+\alpha_h)^2}{d+t}B(\alpha_h,\beta_h)} & \end{cases} \tag{A.9}$$

While the effect of t and d_h on marginal curtailment induce the same change in marginal usable supply, this is not the case for changes in α_h. This is because changes in α_h also affect the level of marginal potential supply ($US_h = PS_h - K_h$). Hence, to access the effect of α_h on the spatial allocation of marginal capacity I also derive the effect on marginal usable supply.

In a first step I derive the effect of α_h on the marginal potential supply:

$$\begin{aligned} PS_h\Big|_{V_h=v} &= v \cdot \frac{\alpha_h}{\alpha_h+\beta_h} \\ \frac{\partial PS_h}{\partial v}\bigg|_{V_h=v} &= \frac{\alpha_h}{\alpha_h+\beta_h} \\ \frac{\partial^2 PS_h}{\partial v \partial \alpha_h}\bigg|_{V_h=v} &= \frac{\beta_h}{(\alpha_h+\beta_h)^2} \end{aligned} \tag{A.10}$$

In a second step I derive $\frac{\partial^2 US_h}{\partial v \partial \alpha_h}\Big|_{V_h=v}$ by subtracting $\frac{\partial^2 K_h^t}{\partial v \partial \alpha_h}\Big|_{V_h=v}$ from $\frac{\partial^2 PS_h}{\partial v \partial \alpha_h}\Big|_{V_h=v}$:

$$\frac{\partial^2 US_h}{\partial v \partial \alpha_h}\bigg|_{V_h=v} = \begin{cases} \frac{\beta_h}{(\alpha_h+\beta_h)^2} & \text{for: } v \leq d_h + t \\ \frac{B_{\frac{d_h+t}{v}}(\alpha_h+1,\beta_h)\left(\log\left(\frac{d_h+t}{v}\right)+\psi^{(0)}(\alpha_h+\beta_h)-\psi^{(0)}(\alpha_h)\right)}{B(\alpha_h,\beta_h)} & \\ \quad - \frac{\left(\frac{d+t}{v}\right)^{\alpha_h} {}_3F_2\left(\alpha_h+1,\alpha_h+1,1-\beta_h;\alpha_h+2,\alpha_h+2;\frac{d+t}{v}\right)}{\frac{v(1+\alpha_h)^2}{d+t}B(\alpha_h,\beta_h)} & \text{for: } v > d_h + t \end{cases} \tag{A.11}$$

For $v > d_h + t$ and valid parameter values (i.e., $\alpha_h, \beta_h, d_h + t > 0$) the term $\frac{\partial^2 K_h^t}{\partial v \, \partial \alpha_h}\Big|_{V_h = v}$ can be positive or negative. This implies that marginal usable supply when marginally increasing v evaluated at $V_h = v$ can either increase at a lower rate or higher rate with increasing α_h.

Appendix B. Historical availabilities for wind and solar in Germany and corresponding Beta distribution

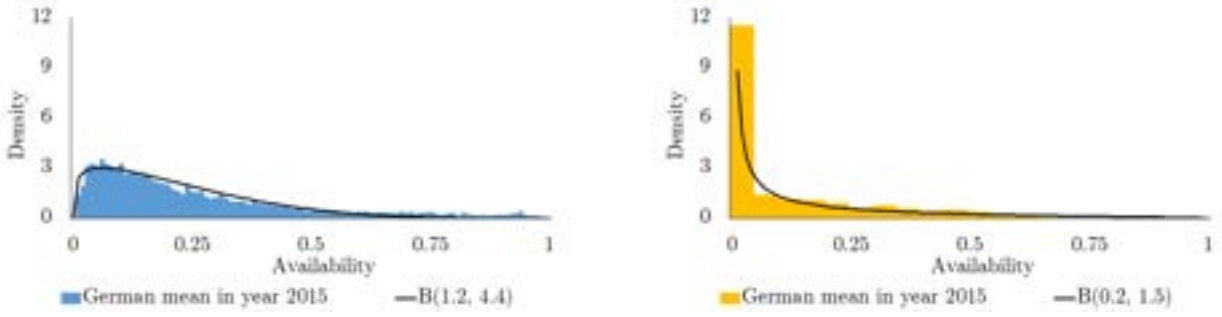

(a) Wind Onshore (b) Solar

Figure B.13: Comparison of historical availabilities for wind and solar in Germany with the corresponding Beta distribution.

Appendix C. Applied and historical densities for wind power

Figure C.14 shows the density of potential supply assumed for the high and low-availability node in all figures of Section 3 and 4 with constant availability distribution parameters (i.e., Figure 2, 3, 4, 5, 8, 9, 10). Additionally, the Figure C.14 displays the density of estimated historical wind power availabilities for the year 2015-2022 in the German market areas TransnetBW and Tennet. The estimation is based on data from the Bundesnetzagentur's electricity market information platform (BNetzA, 2022). TransnetBW is located in the south of Germany, and most wind power plants in the Tennet market area are located in the north. This implies that the availability density parameters in the analysis at hand resemble the availabilities for wind in the north (h) and south (l) of Germany.

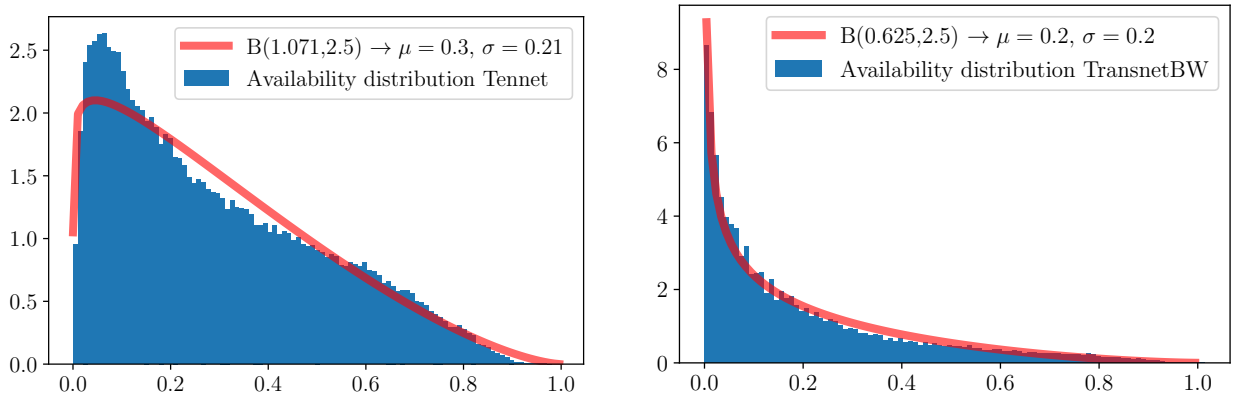

(a) High-availability node

(b) Low-availability node

Figure C.14: Historical availability densities for the years 2015-2022 and in this analysis applied densities.

Appendix D. Description and explanation of formulas used to compute Figures 2-12

The Figures 2-12 are the result of numerical optimisations. In each figure, the optimisation is obtained for 201 different VRE penetration levels (v) ranging from 0 to $6d_{h+l}$, such that the interval between two analysed VRE penetration levels equals $\frac{6d_{h+l}}{200}$.

The optimisation problem solved numerically resembles the optimisation problems I describe in Chapter 3 and 4. For the case of nodal pricing (Chapter 3) I use Equation 8 as objective function. The objective function contains the terms PS_i and K, which both depend on the decision variable V_h.

To calculate the potential VRE supply (PS_i) I apply Equation 4. However, instead of using the beta density function as availability profile, implicitly assuming availability realisations going towards infinity ($n \to \infty$), I use a finite number of availability realisations ($avail_{i,r}$). Thereby r represents the index for different realisations. Considering 10 million periods balances the trade-off between being as close as possible to the underlying beta distribution and allowing for computational feasibility (i.e., $n = 1 \cdot 10^7$). For $n = 1 \cdot 10^7$ the 99%-confidence interval of μ_i is given by $\mu_i \pm 0.0026\sigma_i$.

Like described in Equation 7 curtailment (K) can be separated into K_i^t and K^d. K_i^t is calculated by applying Equation A.1. However, instead of using the exact beta density function (implicitly assuming an $n \to \infty$) I consider 10 million periods which leads to the following function:

$$K_i^t = \frac{1}{n} \sum_r \max \left\{ 0, V_i avail_{i,r} - (d_i + t) \right\} \tag{D.1}$$

K^d occurs, when the global potential supply minus curtailment from limited transmission capacity exceeds

the global demand. The level of K^d is calculated using the following function:

$$K^d = \frac{1}{n}\sum_r max\left\{0, \sum_i \underbrace{V_i avail_{i,r}}_{PS_{i,r}} - \underbrace{\sum_i \max\left\{0, V_i avail_{i,r} - (d_i + t)\right\}}_{K^t_{h,r} + K^t_{l,r}} - d_{h+l}\right\} \tag{D.2}$$

Thereby I consider each of the 10 million periods (i.e., $n = 1 \cdot 10^7$).

For the case of uniform pricing, I use Equation 19 as objective function (Chapter 4). The objective function contains the terms potential supply (PS_i) and commercial curtailment ($\overline{K^c}$). The potential supply is calculated analogue as presented above. The commercial commercial ($\overline{K^c}$) I calculate using the following Equation:

$$\overline{K^c} = \frac{1}{n}\sum_r^n \max\{0, \underbrace{\sum_i V_i avail_{i,r}}_{PS_{h,r} + PS_{l,r}} - d_{h+l}\} \tag{D.3}$$

Like in the case of nodal pricing I consider 10 million periods (i.e., $n = 1 \cdot 10^7$).

Next to solving the problem numerically, I derive several results. First, I calculate the marginal capacity share at node h, which represents how nodal capacity changes with an increase of v. This is done by calculating $\frac{\Delta V_h}{\Delta v}$ with $\Delta v = \frac{6 d_{h+l}}{200}$ using the optima calculated for the 201 VRE penetration levels. Second, I calculate the average capacity share at node h (i.e., $\frac{V_h}{v}$). Third, I show the marginal usable supply and node h and l (i.e., $\frac{\Delta US_h}{\Delta v}$ and $\frac{\Delta US_l}{\Delta v}$). The numbers are calculated by using the following Equation:

$$\frac{\Delta US_i}{\Delta v} = \frac{US|_{v=\overline{v}+\epsilon, V_i=(V_i^*|_{v=\overline{v}})+\epsilon} - US|_{v=\overline{v}, V_i=V_i^*}}{(\overline{v}+\epsilon) - \overline{v}} \tag{D.4}$$

The equation contains ϵ to identify the effect on an incremental increase in the VRE penetration (v). In the numerical simulation I assume $\epsilon = 0.01$. Fourth, the global VRE share is provided, defined by $\frac{\sum_i PS_i - K_i}{d_{h+l}}$. The reduction in global VRE share arising from the inefficient allocation under uniform (while keeping all parameters constant) is provided as well in the figures in Chapter 4. Figure 8 additionally shows the marginal saleable supply at node h and l under uniform pricing (i.e., $\frac{\Delta SS_h}{\Delta v}$ and $\frac{\Delta SS_l}{\Delta v}$). The numbers are calculated by using the following Equation:

$$\frac{\Delta SS_i}{\Delta v} = \frac{SS|_{v=\overline{v}+\epsilon, V_i=(V_i^*|_{v=\overline{v}})+\epsilon} - SS|_{v=\overline{v}, V_i=V_i^*}}{(\overline{v}+\epsilon) - \overline{v}} \tag{D.5}$$

Like in Equation D.4 I assume $\epsilon = 0.01$.

To do the calculations and to generate the figures I applied Python 3.9 using the Packages Scipy 1.9.3

(generating the beta distribution and optimising the problem), Numpy 1.24.0 and Pandas 1.5.2 (data preparation) as well as Matplotlib 3.6 (plotting the figures).

Appendix E. Effect of changing μ_i with the means of α_i on σ_i

The Beta distribution $B(\alpha, \beta)$is defined by the parameter α and β. These parameters define the average and the standard deviation. When changing the average with the means of changing α. The standard deviation remains rather constant.

Figure E.15a) shows the effect of varying μ_i in the interval [0.2,0.5] with the means of changing α_i for the case of $\beta = 4.4$. The density function and the resulting standard deviation are displayed. One can see that the density functions moves, while standard deviation remains rather constant, varying only between 0.2 and 0.22.

Figure E.15b) displays the maximum change in the standard deviation when varying α_i, such that μ_i is varied in the interval [0.2,0.5] for different level of β. One can see, that the maximum change in the variance for $\beta \in [0.5, 40]$ does not exceed 0.04. For $\beta > 2.2$ the maximum change does not exceed 0.02.

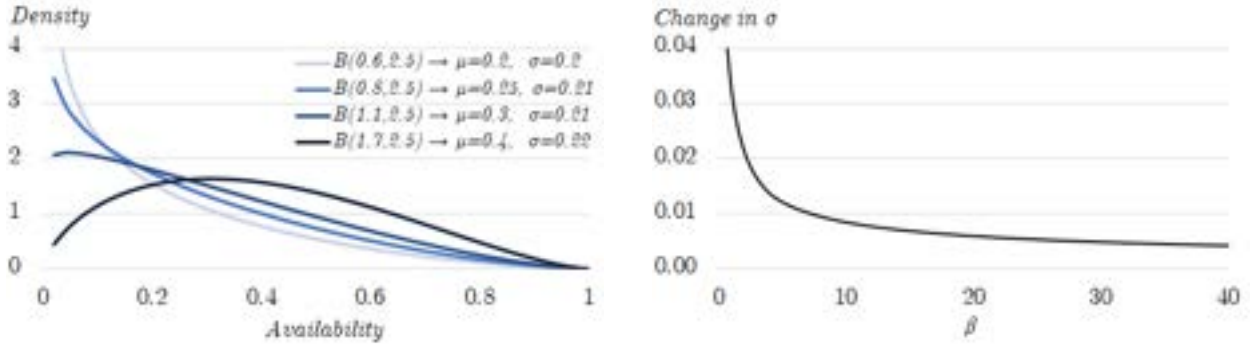

(a) Effect on density

(b) Effect on σ when varying $\mu \in [0.2, 0.5]$

Figure E.15: Effect on σ when changing μ with the means of α.

Appendix F. Effects of the variance on the spatial allocation ranges when transmission capacity is high

Figure F.16 displays the insights from Finding NP 6 numerically for the case of high transmission capacity (i.e., $t = \frac{3}{4}d_i$). Assumptions regarding the demand and the availability profiles are identical to Figure 6. When the variance is increased at node h (compare Figure F.16a and b), the *high-potential deployment range* is shortened from $2.0d_{h+l}$ to $1.4d_{h+l}$. Additionally, the figure confirms that increasing σ_i^2 lowers the nodal capacity share in the *split capacity range* independent of the VRE penetration level.

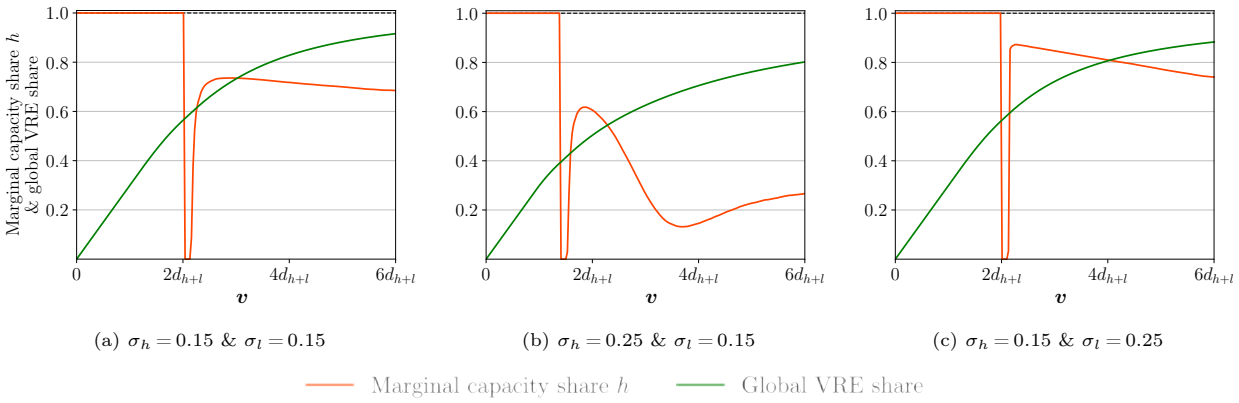

(a) $\sigma_h = 0.15$ & $\sigma_l = 0.15$ (b) $\sigma_h = 0.25$ & $\sigma_l = 0.15$ (c) $\sigma_h = 0.15$ & $\sigma_l = 0.25$

Figure F.16: Effect of the variance in the availability profile on the spatial allocation ranges under nodal pricing.

References

ACER, 2022. Decision No 11/2022 of the European Union Agency for the Cooperation of Energy Regulators of 8 August 2022 on the alternative bidding zone configurations to be considered in the bidding zone review process. URL: https://www.acer.europa.eu/sites/default/files/documents/Individual%20Decisions/ACER%20Decision%2011-2022%20on%20alternative%20BZ%20configurations.pdf.

Bird, L., Lew, D., Milligan, M., Carlini, E.M., Estanqueiro, A., Flynn, D., Gomez-Lazaro, E., Holttinen, H., Menemenlis, N., Orths, A., Eriksen, P.B., Smith, J.C., Soder, L., Sorensen, P., Altiparmakis, A., Yasuda, Y., Miller, J., 2016. Wind and solar energy curtailment: A review of international experience. Renewable and Sustainable Energy Reviews 65, 577–586. doi:10.1016/j.rser.2016.06.082.

BNetzA, 2022. SMARD - Electricity market data for Germany. URL: https://www.smard.de/en.

Cholteeva, Y., 2020. Constraint payments: rewarding wind farms for switching off. URL: https://www.power-technology.com/features/constraint-payments-rewarding-wind-farms-for-switching-off/.

Cialani, C., Mortazavi, R., 2018. Household and industrial electricity demand in Europe. Energy Policy 122, 592–600. URL: https://www.sciencedirect.com/science/article/pii/S0301421518305068, doi:10.1016/j.enpol.2018.07.060.

Czock, B., Sitzmann, A., Zinke, J., 2022. The place beyond the lines - Efficient storage allocation in a spatially unbalanced power system with a high share of renewables, display, Bonn. URL: https://meetingorganizer.copernicus.org/EMS2022/EMS2022-196.html, doi:10.5194/ems2022-196.

Elberg, C., Hagspiel, S., 2015. Spatial dependencies of wind power and interrelations with spot price dynamics. European Journal of Operational Research 241, 260–272. URL: https://linkinghub.elsevier.com/retrieve/pii/S0377221714006614, doi:10.1016/j.ejor.2014.08.026.

Fürsch, M., Hagspiel, S., Jägemann, C., Nagl, S., Lindenberger, D., Tröster, E., 2013. The role of grid extensions in a cost-efficient transformation of the European electricity system until 2050. Applied Energy 104, 642–652. URL: https://linkinghub.elsevier.com/retrieve/pii/S0306261912008537, doi:10.1016/j.apenergy.2012.11.050.

Green, R., 2007. Nodal pricing of electricity: how much does it cost to get it wrong? Journal of Regulatory Economics 31, 125–149. URL: http://link.springer.com/10.1007/s11149-006-9019-3, doi:10.1007/s11149-006-9019-3.

IEA, 2022a. VRE share in annual electricity generation in selected countries, 2016-2022. URL: https://www.iea.org/data-and-statistics/charts/

vre-share-in-annual-electricity-generation-in-selected-countries-2016-2022.

IEA, 2022b. World Energy Outlook 2022. Paris.

Kies, A., Schyska, B., von Bremen, L., 2016. Curtailment in a Highly Renewable Power System and Its Effect on Capacity Factors. Energies 9, 510. URL: http://www.mdpi.com/1996-1073/9/7/510, doi:10.3390/en9070510.

Müller, T., 2017. The Role of Demand Side Management for the System Integration of Renewable Energies, in: IEEE. doi:10.1109/EEM.2017.7981892.

Obermüller, F., 2017. Build wind capacities at windy locations? Assessment of system optimal wind locations , 31.

Pechan, A., 2017. Where do all the windmills go? Influence of the institutional setting on the spatial distribution of renewable energy installation. Energy Economics 65, 75–86. URL: https://linkinghub.elsevier.com/retrieve/pii/S0140988317301457, doi:10.1016/j.eneco.2017.04.034.

Schmidt, L., Zinke, J., 2020. One price fits all? Wind power expansion under uniform and nodal pricing in Germany 20, 44.

Schweppe, F.C., Caramanis, M.C., Tabors, R.D., Bohn, R.E., 1988. Spot Pricing of Electricity. Springer US, Boston, MA. URL: http://link.springer.com/10.1007/978-1-4613-1683-1, doi:10.1007/978-1-4613-1683-1.

Sinden, G., 2007. Characteristics of the UK wind resource: Long-term patterns and relationship to electricity demand. Energy Policy 35, 112–127. URL: https://linkinghub.elsevier.com/retrieve/pii/S0301421505002752, doi:10.1016/j.enpol.2005.10.003.

Sinn, H.W., 2017. Buffering volatility: A study on the limits of Germany's energy revolution. European Economic Review 99, 130–150. URL: https://linkinghub.elsevier.com/retrieve/pii/S0014292117300995, doi:10.1016/j.euroecorev.2017.05.007.

Staffell, I., Pfenninger, S., 2016. Using bias-corrected reanalysis to simulate current and future wind power output. Energy 114, 1224–1239. URL: https://linkinghub.elsevier.com/retrieve/pii/S0360544216311811, doi:10.1016/j.energy.2016.08.068.

Yasuda, Y., Bird, L., Carlini, E.M., Eriksen, P.B., Estanqueiro, A., Flynn, D., Fraile, D., Gómez Lázaro, E., Martín-Martínez, S., Hayashi, D., Holttinen, H., Lew, D., McCam, J., Menemenlis, N., Miranda, R., Orths, A., Smith, J.C., Taibi, E., Vrana, T.K., 2022. C-E (curtailment – Energy share) map: An objective and quantitative measure to evaluate wind and solar curtailment. Renewable and Sustainable Energy Reviews 160, 112212. URL: https://linkinghub.elsevier.com/retrieve/pii/S1364032122001356,

doi:10.1016/j.rser.2022.112212.

Zerrahn, A., Schill, W.P., Kemfert, C., 2018. On the economics of electrical storage for variable renewable energy sources. European Economic Review 108, 259–279. URL: https://linkinghub.elsevier.com/retrieve/pii/S0014292118301107, doi:10.1016/j.euroecorev.2018.07.004.